

AD-A143 465

QUANTUM STRUCTURE OF ADSORBATES ON SEMICONDUCTOR
SURFACES(U) MONTANA STATE UNIV BOZEMAN DEPT OFPHYSICS
G J LAPEVRE DEC 83 AFOSR-TR-84-0584 AFOSR-82-0267

1/1

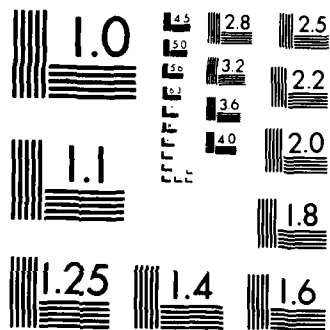
UNCLASSIFIED

F/G 20/10

NL

END

FILMED
...
DTIC



MICROCOPY RESOLUTION TEST CHART
NATIONAL BUREAU OF STANDARDS-1963-A

AD-A143 465

DTIC FILE COPY

REPORT DOCUMENTATION PAGE		READ INSTRUCTIONS HOW TO COMPLETE THIS FORM
1. REPORT NUMBER AFOSR-TR- 84-0584	2. GOVT ACCESSION NO.	3. REPORT DATE
4. TITLE (and Subtitle) QUANTUM STRUCTURE OF ORBITALS ON SEMICONDUCTOR SURFACES	5. AUTHOR(s) Gerald J. Lapeyre	6. PERFORMING ORGANIZATION NAME AND ADDRESS Department of Physics Montana State University Bozeman, Montana 59717
7. CONTROLLING OFFICE NAME AND ADDRESS AF Office of Scientific Research (NE) Building 410, Bolling AFB, D.C. 20332	8. MONITORING AGENCY NAME & ADDRESS (if different from Controlling Office)	9. SECURITY CLASS. of this report Unclassified
10. DISTRIBUTION STATEMENT (of this Report) Approved for public release; distribution unlimited		11. SECURITY CLASS. of this report's ABSTRACT Unclassified
12. DISTRIBUTION STATEMENT (of the abstract entered in Block 20, if different from Report)		13. DECLASSIFICATION/DOWNGRADING SCHEDULE
14. SUPPLEMENTARY NOTES		
15. KEY WORDS (Continue on reverse side if necessary and identify by block number) Photoemission spectroscopy; Electronic structure; Band structure; surface states; Angle-resolved electron emission; Synchrotron radiation; III-V semiconductors; Gallium Arsenide; Germanium arsenide; Chemisorption; and adsorption of oxygen.		
16. ABSTRACT (Continue on reverse side if necessary and identify by block number) See reverse side		

DTIC ELECTE
 JUL 27 1984
 S
 D
 E

- Polarization-dependent angle-resolved photoemission spectroscopy with synchrotron radiation was performed for Fe adatoms on GaAs(110) surface in the monolayer regime. Chemisorbed states at the Γ point in the Brillouin zone were observed about 0.8 eV below the valence band maximum. These states are attributed to chemisorption states that are predicted to exist at the junction interface states which are theoretically predicted.
- A special low temperature UHV manipulator was constructed and used to perform oxygen and CO physisorption experiments on GaAs(110) at about 45° K. The electronic structure of adsorbed oxygen determined by photoemission is essentially that observed for the gas phase which establishes the existence of the molecular physisorbed state. The molecularly adsorbed oxygen converts, upon warming to room temperature, to an atomic chemisorbed state essentially the same as that obtained for room temperature adsorption. These studies were motivated by the problem of finding stable insulating layers on III-V semiconductors.

A. Front Cover

FINAL SCIENTIFIC REPORT
FOR
QUANTUM STRUCTURE OF ADSORBATES
ON SEMICONDUCTOR SURFACES



Author: Gerald J. Lapeyre
Principal Investigator
Professor, Department of Physics
Montana State University
Bozeman, Montana 59717

Accession For	
NTIS CRA&I	<input checked="" type="checkbox"/>
DTIC TAB	<input type="checkbox"/>
Unannounced	<input type="checkbox"/>
Justification	
By _____	
Distribution/ _____	
Availability Codes	
Avail and/or	
Dist	Special
A-1	

Report Period: 1 July 1982 - 31 December 1983
Start Date: 1 July 1982
Research Grant Number: AFOSR-82-0267
Project Task Number: 2306/B1

Contents of Report

- A. Front Cover
- B. Description of Grant Effort and Results
- C. Publications Resulting from AFOSR Support
- D. Professional Personnel
- E. Coupling

Research sponsored by
United States Air Force Office of Scientific Research

Approved for public release; distribution unlimited.

B. Description of Grant Effort and Results

The study performed experimental investigations on the fundamental nature of adatoms on compound (III-V) semiconductor surfaces. The method used was polarization-dependent angle-resolved photoemission (PARPES) with synchrotron radiation and resonance lamp angle-integrated UV photoemission (IUP). Photoemission measures the electronic structure of a sample. The specific adatoms were oxygen, carbon monoxide, and germanium on the cleaved faces of GaAs(110).

Germanium on Gallium Arsenide

The Ge/GaAs system is both technologically and scientifically interesting; it is the basis of a technologically important heterojunction and provides an example of how an adatom which normally forms a tetrahedrally bonded crystal behaves on a compound semiconductor surface. One expects Ge in the monolayer regime to form "surface states" which are precursors to heterojunction interface states, and such had been theoretically predicted.^{1,2} We observed for the first time such states near the point in the Brillouin zone about 5.8 eV below the valence band maximum. The states which were weak corresponded to some of the theoretically predicted states. The experimentation necessary to find such induced states is sophisticated and requires extensive work, largely because of the complicated wave vector dependence of the states throughout the Brillouin zone. The search for such states is further complicated by the numerous interband band transitions characteristic of III-V crystals which are present in

AIR FORCE OFFICE OF SCIENTIFIC INFORMATION
NOTICE
This technical report is available to the
public through the National Technical Information Administration
approx. \$10.00 per copy
2
MATTHEW J. R. [unclear]
Chief, Technical Information Division

the photoemission spectra. A detailed assignment to specific interband transitions which had been largely worked out under support from a previous grant proved to be most valuable for interpreting the data on the germanium overlayers. Because of the complications mentioned above one cannot conclude at this time whether or not the lack of observing all predicted states is a weakness in the theoretical model. A report of these observations did stimulate some additional calculations, although considerable additional work needs to be done in this area.

The behavior of adatoms on compound semiconductor surfaces is also complex because structural changes may occur. Some adatoms may move into the substrate, and some substrate atoms may move out. Such phenomena is observed for the Ge/GaAs system. For example, annealing of a few monolayers of Ge produces a (3x1) LEED pattern instead of the (1x1) pattern which may be obtained by moderate annealing in the low coverage cases. The latter structure is that used in the above mentioned theoretical models. In addition to the (3x1) pattern observed for higher temperature anneals, one finds that the surface contains an excess of As. One postulated model for the (3x1) structure is that it is very similar to a given layer in the layered crystal GeAs. Hence, ARPES studies were performed on GeAs crystals and the experimental electronic structure was obtained. It contains a large number of very flat bands which are typical of layered material. Theoretical electronic structure calculations needed for further interpretation are not yet available.

Oxygen on Gallium Arsenide

The absorption of small atmospheric molecules on compound semiconductor surfaces is an important area of study. In particular, oxygen is likely to play a vital role in the formation of stable insulating films on GaAs. Previous studies of oxygen have been complicated by the fact that the initial adsorption probability is approximately one in a million, which means that surface defects and/or gas contamination may play an important role in chemisorption experiments. To avoid this problem the GaAs crystals were cooled to low enough temperatures to obtain essentially unity sticking coefficient for oxygen. We performed the first studies employing low temperature adsorption (physisorption) and then observed the evolution of the GaAs-oxygen system that occurred as the temperature was increased. In these experiments the crystals were allowed to warm to room temperature. The angle-integrated photoemission experiments were performed with a resonance lamp. Physisorption was successfully obtained at about 45° K as demonstrated by the observation of structures in the photoemission spectra which are essentially the same as the gas phase spectra. As is typical in physisorption the gas phase structures are broadened and shifted due to the binding process, but all the lines are observed at essentially the gas phase spacing. Upon warming to room temperature, some oxygen is desorbed, but approximately one fourth is retained and the electronic structure is essentially the same as that observed for room temperature adsorption. Room temperature adsorption is attributed to atomic chemisorption. The dramatic change in

ring in our spectra support the latter interpretation. Upon warming to room temperature at least one intermediate state was observed, but time limits prohibited further studies. More detailed temperature-dependent studies along these lines need to be performed as well as PARPES studies with synchrotron radiation.

Because CO is always present in an experimental chamber as well as in the atmosphere, one study of CO was performed to determine its photoemission spectra. We found no interaction between the oxygen and CO in these studies and were so able to separate out the structures in the photoemission spectra due to CO. We found that CO molecularly adsorbs at the same temperature that we adsorb the oxygen, but we found that CO, within the sensitivity of our measurements (approximately one percent), completely desorbs upon warming to room temperature. At low coverages (\leq a quarter monolayer), the CO photoemission spectra is significantly different from the gas phase spectra while larger coverages of around a monolayer give spectra more like that from the gas phase CO except that not all the lines are uniformly shifted with respect to the vacuum level (ionization limit). The observation of the precursor state for this adsorption system is rather interesting but was not pursued in these studies. However, we did look for a precursor state for the oxygen adsorption and found none. (We note that we did not carry these studies down to the level of approximately 1/100 of a monolayer, which should be done.) It is worth commenting that oxygen which does interact with the substrate upon warming does

not show a precursor state, *i.e.* modification of the molecular gas phase states, while the GaAs(110) surface will interact enough to modify the CO states even though CO desorbs before forming a chemisorbed state. One would expect that further studies of the oxygen intermediate species occurring in the evolution of low temperature physisorbed state to the room temperature chemisorbed oxygen as well as further studies of the CO system would bear on the nature of these interactions.

SUMMARY

Specific experimental results were obtained for two important classes of adatoms on GaAs. In addition to demonstrating that heterojunction type interface states are observable, the studies point to several new areas of study. One is that new phenomena are obtained by low temperature "induced" adsorption with subsequent heating. Another is that Ge adsorption which, in a broad sense of the word is just one example of a group III, VI, V atoms, causes changes in the substrate band structure. These effects were obtained from data taken under the sponsorship of this grant but analyzed under the support of other grants. To our knowledge such behavior has not been reported or alluded to in the literature, and we predict its consequences in the areas of heterojunctions and Schottky barriers will be very important.

REFERENCES

1. W.E. Pickett, S.G. Louis, and M.L. Chohen, Phys. Rev. Lett. **39**, 109 (1977); W.E. Pickett and M.L. Cohen, J. Vac. Sci. Technol. **15**, 2437(1978)
2. A. Masur, J. Pollman, and M. Schmeitz, Solid State Commun. **36**, 961 (1980); C.A. Swartz, W.A. Goddard III, and T.C. McGill, J. Vac. Sci. Technol. **19**, 551 (1981).

C. Publications Resulting from APOSP Support

1. Research Journal Articles

"Adsorption of O₂ and CO on Cleaved GaAs(110) at Low Temperatures", D.J. Frankel, Y. Yukun, R. Avci, G.J. Lapeyre. J. Vac. Sci. Technol. A1(2), 679 (1983).

"UV Photoemission Study of Low Temperature Oxygen Adsorption on GaAs(110)", D.J. Frankel, J. Anderson, and G.J. Lapeyre. J. Vac. Sci. Technol. B13, 763 (1983).

"Photoemission Study of GeAs(201): A Model for the As-Stabilized Ge Surface on GaAs/Ge Heterojunctions", F. Stucki, G.J. Lapeyre, R.S. Bauer, P. Zurcher, and J.C. Mikkelsen, Jr. J. Vac. Sci. Technol. B1(4), 865 (1983).

"Observation of Nonuniform Energy Band Shifts for Ge on GaAs(110)", P. Zurcher, J. Anderson, D. Frankel, and G.J. Lapeyre. Physica 117B and 118B, 857 (1983).

2. Invited Conference Papers

"Chemisorption Problems for Compound Semiconductor Surfaces", G.J. Lapeyre. Materials Research Society Annual Meeting, Boston, 1983 (contained some results from this study)

3. Contributed Conference Papers

"Adsorption of O₂ and CO on Cleaved GaAs(110) at Low Temperatures", D.J. Frankel, Y. Yukun, and R. Avci and G.J. Lapeyre. 29th National American Vacuum Society Symposium, Baltimore, November 1982.

"UV Photoemission Study of Low Temperature Oxygen Adsorption on GaAs(110)", D.J. Frankel, J. Anderson, and G.J. Lapeyre. 10th Annual PCSI Conference, Santa Fe, January 1982.

"Photoemission Study of GeAs(201): A Model for the As-Stabilized Ge Surface on GaAs/Ge Heterojunctions", F. Stucki, R. Bauer, J.C. Mikkelsen, Jr., and G.J. Lapeyre. 10th Annual PCSI Conference, Santa Fe, January 1982.

"Observation of Non Uniform Energy Band Shifts for Ge on GaAs(110)", P. Zurcher, J. Anderson, D.J. Frankel, and G.J. Lapeyre. 16th International Conference on the Physics of Semiconductors, Montpellier, France. September 1982.

"Observation on Non Uniform Energy Band Shifts for Ge on GaAs(110)", P. Zurcher, J. Anderson, D. Frankel, and G.J. Lapeyre. International Conference on Semiconductors in the Vacuum UV: Application of Synchrotron Radiation, Berlin, W. Germany. September 1982.

D. Professional Personnel

Principal Investigator

Gerald J. Lapeyre
Professor of Physics

Post-doctoral Research Associates (partial support)

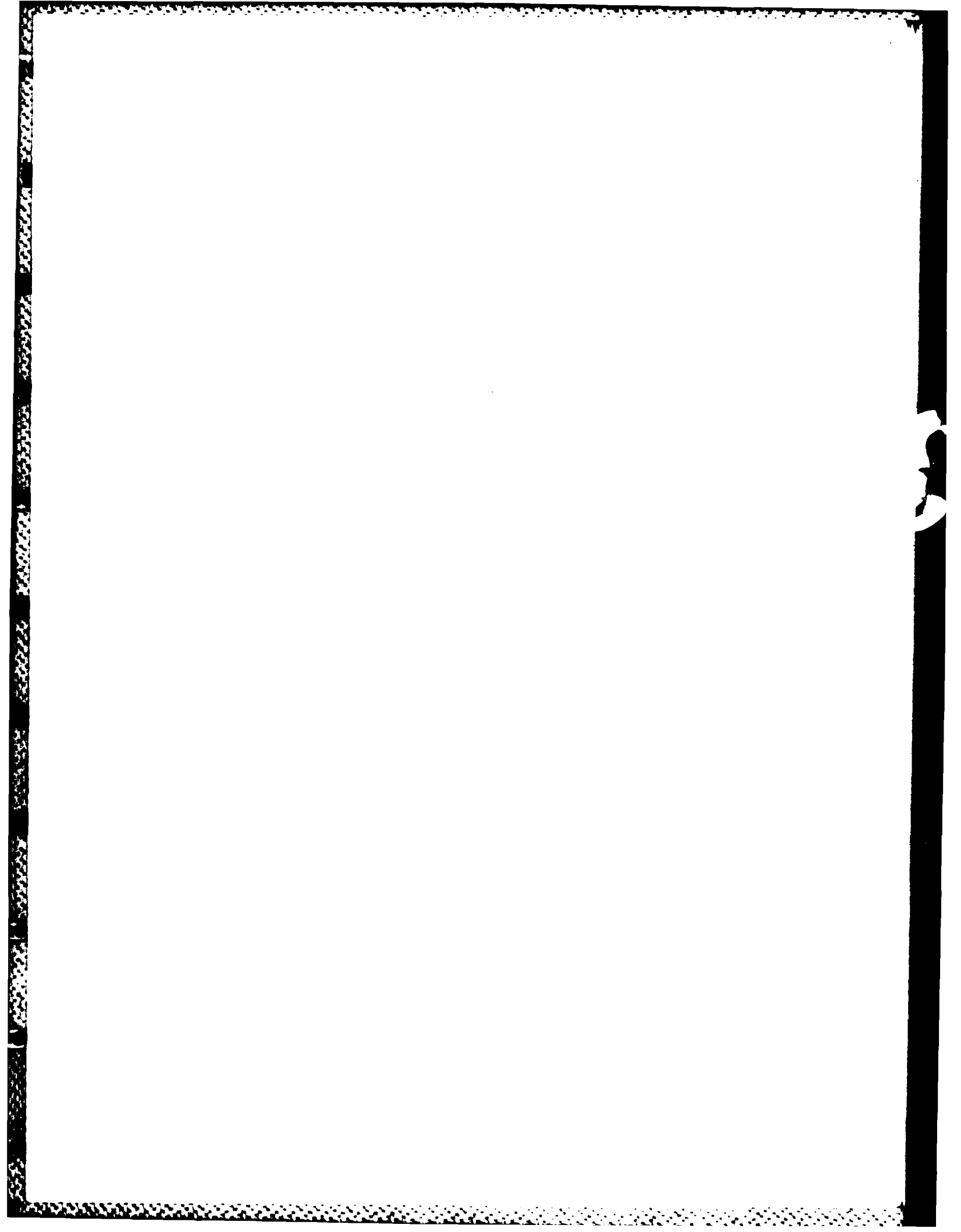
James R. Anderson
Franz Stucki
David J. Frankel

Research Assistants (partial support)

James R. Myron
Mark Dickson

E. Coupling

1. The investigations on GeAs were done in collaboration with R.S. Bauer's group from Xerox Corporation, which was partially supported by the Office of Naval Research.
2. Presented paper at the 1982 "Annual Synchrotron Radiation Users Meeting" at the University of Wisconsin, Synchrotron Radiation Center in Stoughton, Wisconsin.
3. Seminars given at the following laboratories:
University of Notre Dame



OBSERVATION OF NONUNIFORM ENERGY BAND SHIFTS FOR Ge ON GaAs(110)

P. Zurcher,* J. Anderson, D. Frankel, and G.J. Lapeyre

Department of Physics, Montana State University
Bozeman, Montana 59717

Fractional monolayer studies of Ge on GaAs(110) were performed with angle-resolved photoemission at the Wisconsin Synchrotron Radiation Center. Normal emission data for $14 < h\nu < 27$ eV were analyzed. The most significant effects of the Ge adatoms are shifts in photoemission peaks known to be due to GaAs interband transitions. The shifts, which are nonuniform, are due to specific nonuniform shifts in interband transitions. Valence band (VB) shifts relative to the VB maximum can be determined from some of the transitions. The top VB shifts downward and the next deeper VB shifts upward in the neighborhood of one-third the distance from Γ to X on the Σ line (0.57 \AA^{-1}). We suggest the shifts are the result of chemisorption-induced charge transfers whose resonance-like states decay over several atomic layers below the surface.

I. INTRODUCTION

Polarization-dependent angle-resolved photoemission (PARPES) has been performed on fractional monolayer (ML) coverages of Ge on the cleaved surface of GaAs(110). The experiments emphasized normal emission studies in which the spectra display a number of peaks which for the clean case are all consistent with interband transitions occurring on the sigma line between the gamma and the X point of the bulk zone. While the overall shape of the spectra are not drastically changed, several effects induced by the Ge are noted in normal emission spectra. 1) A chemisorption induced state which is attributed to a precursor state for a heterojunction interface state is observed at a binding energy of 6.8 eV.¹ The state whose properties are discussed elsewhere¹ shows no dispersion (binding energy changes with photon energy changes). 2) Several new peaks appear which show dispersion and agree with the band structure.¹ 3) All the peaks which are present in the clean spectra show shifts induced by the Ge coverage. The size of these shifts for spectra measured at various photon energies exhibit different values. This paper focuses on the characterization and analysis of these peak shifts.

Shifts of the EDC's resulting from the presence of adatoms are frequently observed and are attributed to band bending.²⁻⁷ Such studies, typically based on partially angle-integrated spectra, assume, usually implicitly, that the bands all shift by the same amount. The data obtained in this study show that this situation does not exist in PARPES where individual interband transitions are discernable. This suggests that new perspectives need to be developed for the use of photoemission in the study of surface Fermi-level pinning.

II. EXPERIMENTAL

Samples were prepared by cleaving p-type single crystals⁸ in ultra high vacuum, depositing the Ge films at room temperature and annealing the crystals at about 330°C for a few minutes. The annealing restored the primitive 1x1 LEED pattern of the clean surface with some enhancement of the background. In addition, the angle-resolved spectra show anisotropies, a further indication of order. The film thicknesses were monitored with a quartz crystal thickness monitor and by observing the Ge 3d photoemission spectra. The data were obtained at the Wisconsin Synchrotron Radiation Center.

III. THE DATA AND ANALYSIS

Normal emission energy distribution curves (EDC's) were obtained for photon energies, $h\nu$ between 14 and 27 eV for several specific polarization geometries. The initial energy (binding energy) for all peaks in the EDC's were evaluated with respect to the Fermi level, E_F , which was determined from an evaporated Au film. Changes in peak positions in EDC's can be determined to about 0.05 eV, depending to some extent on the shape of the peak. In those cases where the peak position was difficult to determine, the data point is placed in parentheses. A set of such data for 1/2 ML Ge is shown in the structure plot of Fig. 1. Using spectra which exhibited significant emission from the valence-band-maximum (VBM) region we determined a value for the VBM for the clean and Ge covered surfaces. A value of 0.5 eV is obtained for the VBM shift. Also, the shift of the Ga 3d core was noted, and found to be about 50 meV smaller than the VBM shift. For analysis purposes it is instructive to use a structure plot in which the binding energies are plotted with respect to the VBM, i.e., the Ge:GaAs data is shifted by 0.50

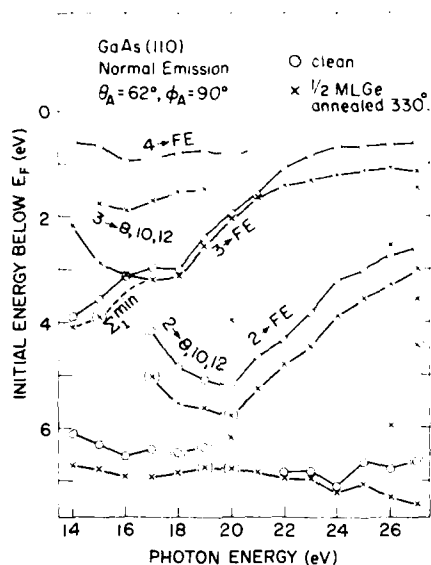
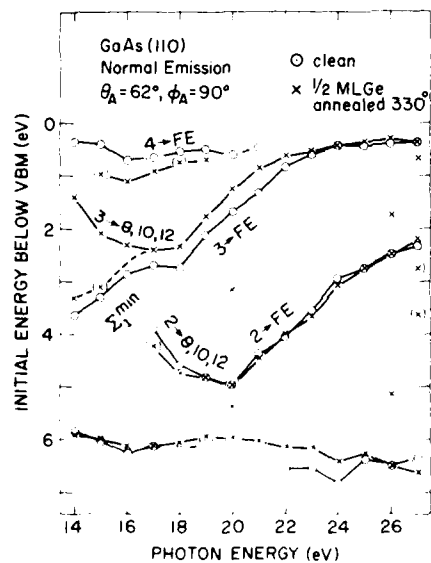
Fig. 1 Structure plot referenced to E_F .

Fig. 2 Structure plot referenced to the VBM.

eV. The resulting structure plot is shown in Fig. 2. One notes that different interband transitions exhibit different shifts. Further, the shift for a given band changes with photon energy. Similar observations and analyses were made for several overlayers on several different cleaved surfaces. Also, shifts of the same general character are observed in the spectra before the Ge overlayer is annealed.

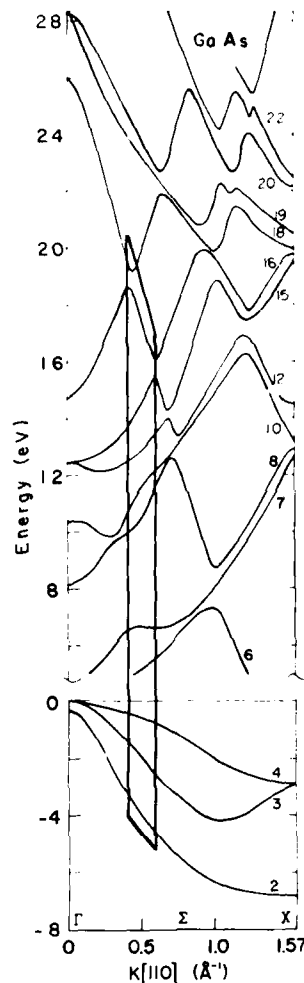


Fig. 3 Bands for the sigma line after Ref. 9.

The photon energy dependences of the binding energies are typical of interband transitions which occur at various values of the perpendicular wave vector, k_{\perp} , depending on the photon energy. The identification of all peaks in normal emission spectra in terms of specific interband transitions at their appropriate k_{\perp} values have been previously determined,⁹ hence we are able to assign specific transitions to the peaks that are observed to shift. The transitions relevant to this paper are noted in Figs. 1 and 2. In Fig. 3 we show the band structure along the sigma line which is the portion of the bulk zone sampled by normal emission.⁹ The band ordering at the X point is chosen for the band labeling sequence. For clarity the odd conduction bands (CB's) which do not photoemit⁹ are deleted, and for convenience

those portions of the CB's derived from the free electron parabola are referred to as the free electron band (FE). In those portions of the zone where the CB's are close together, each CB label is given since the experiment does not resolve such states.

The shifts observed in the EDC's resulting from adsorption can be related to the band structure. We focus here on only those VB transitions to the free electron band. The transitions near the labels 2 to FE, 3 to FE, and 4 to FE in Figs. 1 and 2 all occur around one third of k_x . The domain of these transitions is noted by the "box" in Fig. 3. ($k_x = 0.57 \text{ \AA}^{-1}$ occurs for band 2, 3, 4, at about $h\nu = 17, 19, 21 \text{ eV}$, respectively.) Since the three transitions are all to the same final band the observed shifts reflect relative shifts in the valence bands. The relative shifts as displayed in Fig. 2 are about 0.30 eV downward for VB 4, 0.40 eV upward for VB 3, and 0.10 eV downward for VB 2 for those interband transitions occurring in the box noted on the bands of Fig. 3. The latter values are an average obtained from EDC's for photon energies at 16-18 eV for VB 4, 18-21 eV for VB 3, and 21-24 eV for VB 2. One notes, that as the photon energy increases, the VB to FE transitions "move" toward gamma, and as this occurs the shifts, as plotted in Fig. 2, tend to zero, as expected since the data are referenced to VBM.

IV. DISCUSSION

Typically in photoemission studies on overlayer systems one finds new peaks in the spectra on which one focuses to study the quantum structure of overlayers. The results of this study, however, indicate that one of the primary effects of adding Ge to GaAs is the nonuniform shifts of GaAs interband transitions which show significant dispersion. It is significant to find dispersion connected to effects induced by an overlayer. For the specific transitions discussed here the nonuniform changes in the shifts can be uniquely attributed to the VB's. However, the shifts of other transitions not discussed in this paper seem to also require some relative nonuniform shifts in the CB's. A useful point of view is that the "new states" resulting from the Ge are surface resonances which decay exponentially into the crystal. The decay length is great enough to permit the bulk bands, as probed by photoemission, to manifest the effects of the overlayer-induced resonances. The Ge modifies the charge densities of the tetrahedral bonds in the surface region in such a way that, in some given portions of the zone, each VB has a different shift. Model calculations which contain the atomic orbital character of the band as a function of k and that describe the features

noted here should provide insight as to what features into the quantum structure of the overlayer are important in the calculation of the EDC's in semiconductors.

Photoemission is an important tool for studying band bending. The data reported here indicate that some care is required in interpreting such studies. We see no criterion which defines a special point in k space which can be used for the determination of macroscopic band bending at semiconductor surfaces with methods such as photoemission that sample a region comparable with the region affected by chemisorption induced charge transfer reactions. We suggest that the proper value for band bending is some average of the shifts over all the bands. This may be most easily accomplished in studies which integrate over a significant portion of the emission angles. It appears for this data, as displayed in Fig. 2, that the observed shift for the VBM is close to the average shift of all the bands.

ACKNOWLEDGEMENT: We appreciated several discussions with J. Chadi, E. Bauer, and J. Hermanson, and M. Dickson's aid in the data analysis. The support of the staff at the Wisconsin Synchrotron Radiation Center is appreciated. The research is supported by AFOSR under Contract No. 549620-77-0125 and Grant No. 82-0267, and UWSRC is supported by NSF Grant No. DMR-7415089.

*Presently at Palo Alto Xerox Research Center.

- [1] P. Zürcher, G.J. Lapeyre, J. Anderson, and D. Frankel, *J. Vac. Sci. Technol.* **21**, in press.
- [2] E.A. Kraut, R.W. Grant, J.R. Waldrop, and S.P. Kowalczyk, *Phys. Rev. Lett.* **44**, 1620 (1980).
- [3] P. Perfetti, D. Denley, K.A. Mills, and E.A. Shirley, *Appl. Phys. Lett.* **33**, 667 (1978).
- [4] G. Margaritondo, G. Stoffel, A.D. Katnani, H.S. Edelman, and C.M. Bertoni, *J. Vac. Sci. Technol.* **18**, 784 (1981).
- [5] P. Skeith, I. Lindau, P.W. Zhye, C.Y. Su, and W.E. Spicer, *J. Vac. Sci. Technol.* **16**, 1143 (1979).
- [6] G. Gant and W. Mönch, *Appl. Surf. Sci.*, in press.
- [7] W. Mönch, E.A. Bauer, H. Gant, and R. Marszhall, *J. Vac. Sci. Technol.* **21**, in press.
- [8] The crystals are Zn doped ($3.1 \times 10^{18} \text{ cm}^{-3}$) from Laser Diode.
- [9] F. Cerrina, G.P. Williams, J. Anderson, R.J. Smith, J. Hermanson, J.A. Knapp, and G.J. Lapeyre, to be published; and G.P. Williams, et al., proceedings of this conference. These studies used the bands by K.C. Pandey and by J.R. Chelikowsky and M.L. Cohan.

Adsorption of O₂ and CO on cleaved GaAs (110) at low temperatures^{a)}

D. J. Frankel, Y. Yukun,^{b)} R. Avci,^{c)} and G. J. Lapeyre

Department of Physics, Montana State University, Bozeman, Montana 59717

(Received 27 September 1982; accepted 17 November 1982)

We have studied the low-temperature (~ 50 K) adsorption of O₂ and CO on GaAs (110) with UV photoemission. Spectra were taken using a He discharge lamp and a double pass cylindrical mirror analyzer (CMA) in the angle-integrated mode. Spectra showing peaks characteristic of gas-phase O₂ and CO were observed after dosing GaAs (110) surfaces cleaved at a temperature $T \cong 50$ K with < 5 L of O₂ or CO. The molecular CO peaks disappeared on warming the sample to 100 K leaving a spectrum characteristic of the clean surface. In the case of O₂, the O₂ $1\pi_g$ orbital was 5.4 eV below the valence band maximum (VBM) and 13.2 eV above the Ga $3d$ core, which implies a relaxation shift towards smaller binding energies of ~ 1.4 eV for adsorbed O₂ as compared to the gas phase. On warming the O₂-dosed sample the molecular peaks disappeared by ~ 60 K and by 300 K the spectrum was transformed to one characteristic of chemisorbed oxygen. Auger analysis indicated that oxygen concentrations of a few percent remained at 300 K after O₂ dosing with only 10–40 L at 50 K. The 300 K spectra are attributed to atomic rather than molecular oxygen, which implies a transition from the physisorbed molecule to the chemisorbed atom.

PACS numbers: 68.45.Da, 82.80.Pv, 82.65.My, 79.20.Fv

I. INTRODUCTION

GaAs and in particular the oxidation of GaAs surfaces has been the subject of intensive study.^{1–10} The previous work has shown that there is a very low sticking coefficient for oxygen on GaAs (110) at 300 K, exposures of 10⁶ L or more being required to produce significant coverages of oxygen on the surface. Presently it is generally thought that oxygen dissociates on defect sites and chemisorbs atomically at 300 K. Oxide formation is observed only when hot filaments generate excited oxygen. However, there remains some question as to the exact nature of the oxygen–GaAs bonding in the chemisorbed state. In this article we study the low temperature physisorption of the small molecules CO and O₂, and the evolution of the physisorbed states as temperature is increased, with the aim of understanding better the details of the oxidation process of GaAs (110). We are not aware of any previous studies involving the low temperature adsorption of CO and O₂ on cleaved GaAs (110), although a number of such studies have been carried out on metal surfaces.^{11–15}

II. EXPERIMENTAL EQUIPMENT AND PROCEDURES

Experiments were carried out in a stainless steel ion-pumped vacuum chamber with a base pressure of $\sim 2 \times 10^{-10}$ Torr. The chamber was fitted with a single pass cylindrical mirror analyzer (CMA) and coaxial electron gun for Auger analysis, quadrupole residual gas analyzer (RGA), UV source modeled after the design of Lancaster *et al.*,¹⁶ and a double pass CMA to analyze the photoemitted electrons. A special manipulator coupled to a closed cycle refrigerator allowed the sample to be moved to the various working points in the chamber while being cooled to 40–50 K. Sample temperature was monitored with a Au–0.07% Fe vs chromel thermocouple attached to the sample holder. The sample was *p*-type Zn-doped GaAs (110) from Laser Diode Laboratories with a carrier density $N \sim 3 \times 10^{18}/\text{cm}^3$.

Oxygen exposures were accomplished by filling a thermocouple-gauged prechamber with a measured amount of O₂ (usually 1–10 mTorr), and injecting this dose of oxygen into the main chamber. Since the ion gauge was necessarily off during the actual experiments, absolute values of exposures are only known to within $\sim 30\%$. CO dosing was done through a conventional leak valve with the main chamber pressure monitored with a cold cathode gauge.

UPS spectra of the clean and O₂- or CO-dosed surface were obtained after cleaving at $T = 50$ K. The refrigerator could then be turned off and spectra obtained as the sample gradually warmed up. Because Auger analysis was found to affect drastically the UPS spectra, it was generally carried out only at the conclusion of a run. To avoid the effects of excited oxygen^{2,3} all hot filaments were kept off except during separate calibration experiments.

The chamber pressure rose into the mid 10^{-9} Torr range when the UV source was operating. However, the RGA indicated that the partial pressure of H₂O, CO, and other active gases, remained at the 10^{-10} – 10^{-11} Torr level. During the oxygen dosing process the sample was necessarily exposed to a small amount of CO. RGA measurements showed that each dose of oxygen was accompanied by a pulse of CO roughly 100 times smaller. In addition, during the oxygen dosing and measuring process the background pressure of CO generated an exposure of the order of a few tenths of a langmuir.

III. OXYGEN EXPERIMENTS

An angle-integrated He-II energy distribution curve (EDC) of low temperature-cleaved GaAs (110) is shown in curve 1 of Fig. 1. Features due to four of the resonance lines of the He lamp ($h\nu = 21.2, 40.8, 48.4, 51$ eV) are evident. Also shown in Fig. 1 are difference curves between the clean spectrum and a spectrum obtained after a 4-L exposure to

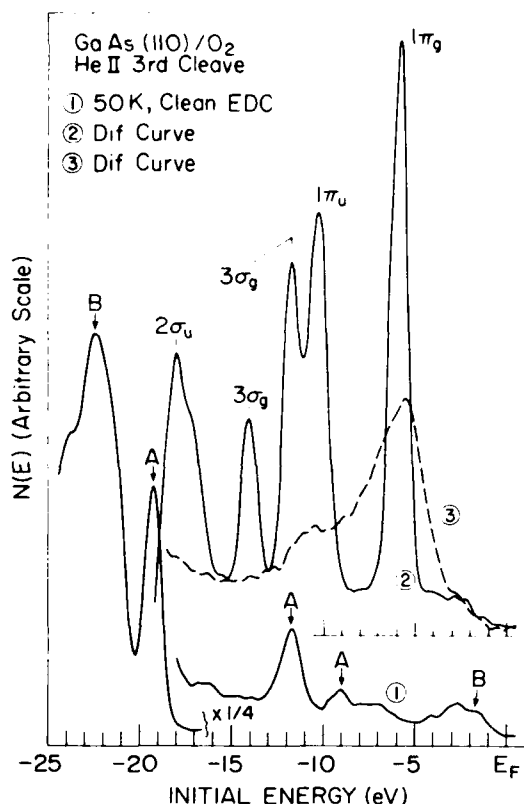


FIG. 1. Curve 1; He-II EDC of clean GaAs (110). Feature A: Ga 3d core excited by 40.8, 48.4, and 51 eV light. Feature B: first valence band of GaAs excited by 21.2 eV (He-I) and 40.8 eV (He-II) light. Curve 2; difference curve, EDC obtained after 4.2 L O₂ exposure at 50 K minus clean EDC. Curve 3; difference curves EDC obtained after exposing sample to 28 L O₂ at 50 K and warming to 300 K minus clean EDC. Note broad 5-eV peak characteristic of chemisorbed atomic oxygen.

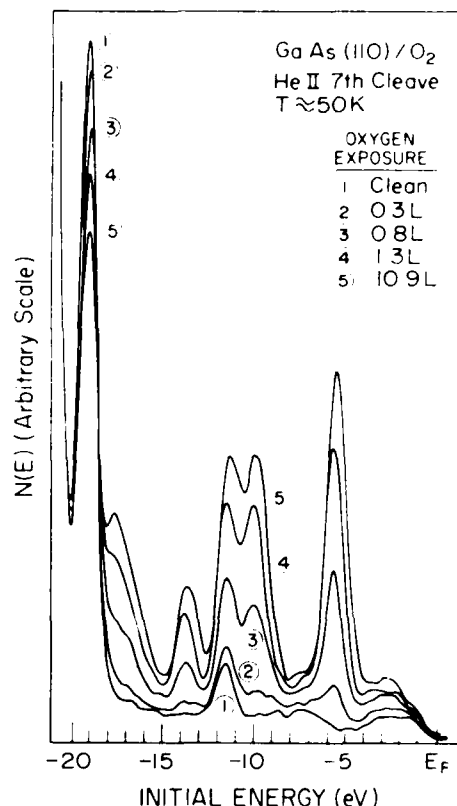


FIG. 2. He-II EDC's showing the effect of a sequence of O₂ exposures at $T = 50$ K. Note broadening to right in the O₂ peaks of curve 5.

oxygen at ~ 50 K, and between the clean spectrum and one obtained after the sample exposed to 28 L of O₂ at 50 K was warmed to 300 K. Difference curves 2 and 3 were calculated by scaling the data to obtain equal count rates at the Ga 3d core before subtraction. In the case of curve 3 the shift in the Fermi level (E_F) upon oxygen chemisorption required that the clean spectrum be shifted by 0.4 eV toward deeper binding energies to align the Ga 3d core levels before subtraction. The spacings of the oxygen peaks in difference curve 2 correspond within 0.1 eV to those of gas phase O₂.^{17,18} The broad peak near 5 eV in curve 3 resembles the structure attributed to chemisorbed atomic oxygen in previous room temperature studies,^{2,3,7,8} and in synchrotron radiation studies by our own group.

Figure 2 shows a series of He-II EDC's obtained as the surface cleaved at 50 K is exposed to increasing amounts of oxygen. The molecular oxygen peaks are first evident at an exposure of $\sim 1/3$ L and saturate after exposures of 2–4 L. A small shift in the Ga 3d core of ~ 0.1 eV towards E_F is evident after the 1/3-L exposure. Additional exposures cause further attenuation of the core, but no additional shift. The position of the valence band maximum (VBM), though difficult to measure to better than 0.1–0.2 eV, appears to remain fixed with respect to E_F during the oxygen adsorption. The modest attenuation ($\sim 20\%$ at saturation) of the Ga 3d core

feature and the low exposure levels indicate that the thickness of the oxygen adlayer is the order of a monolayer. The oxygen peak heights decrease 10%–20% within 20–30 min after dosing, indicating the desorption of some of the weakly bound oxygen molecules, or possibly their conversion to another state. At $T = 45$ –50 K the sample temperature is still well above the condensation temperatures of 23–30 K for O₂ and CO at pressures of 10^{-7} – 10^{-11} Torr.¹⁹

The sequence of events observed after turning off the refrigerator and allowing the sample to slowly warm is fairly complicated and not fully understood at this time. However, the following observations can be made:

- (1) The strong molecular oxygen peaks disappear by 60 K.
- (2) The Ga 3d core level and the position of the VBM remain essentially unchanged during this initial desorption. The Ga 3d core then increases in height and shifts away from the Fermi energy as the temperature is increased from 70 to 300 K, showing a net shift of 0.3–0.5 eV towards greater binding energy as compared to the cold-cleaved and still undosed case. A similar 0.3–0.5 eV shift is seen in the VBM.
- (3) Increases in the 5 eV region characteristic of chemisorbed oxygen occur in the 100–150 K temperature range resulting in the broad chemisorbed oxygen peak.
- (4) Auger measurements at 300 K after oxygen exposures at $T = 50$ K of 10–40 L show concentrations of 2%–3% oxygen on the surface.

During the warming process oxygen and CO are liberated. In control experiments with the RGA and ion gauge the main chamber pressure does not exceed 4×10^{-8} Torr dur-

ing warming and the total exposure to desorbing CO and O₂ is less than 5 L above background. However, effects on the EDC's due to exposure to CO during O₂ dosing and to CO and O₂ during warmup cannot be completely ruled out. In order to further explore these issues we have undertaken the low temperature CO exposure experiments described in the following section.

IV. CO EXPERIMENTS

Figure 3 shows the effects of a series of CO exposures on a GaAs (110) surface cleaved at $T = 50$ K. Strong peaks attributable to physisorbed CO are evident. With the exposure methods used, no significant differences in the rate of growth and the saturation exposure levels for the O₂ and CO features were observed. However, for CO the adsorption/desorption process occurs in two stages. After 0.6 L a low coverage structure is observed that causes a 10%–15% attenuation and a 0.1 eV shift of the Ga 3*d* core level. With exposures of 1.2 L or more a second, higher coverage structure is observed. In this weakly bound state there is a 40%–50% attenuation but no further shift of the Ga 3*d* core. This attenuation is roughly twice the maximum attenuation observed with oxygen.

Figure 4 shows the sequence of the EDC's obtained when the CO exposed sample is allowed to warm up. The high coverage peaks disappear by 60 K. However, a structure identifiable with the low coverage state persists up to 80–100 K. Above this temperature the spectra closely resemble those of the clean surface.

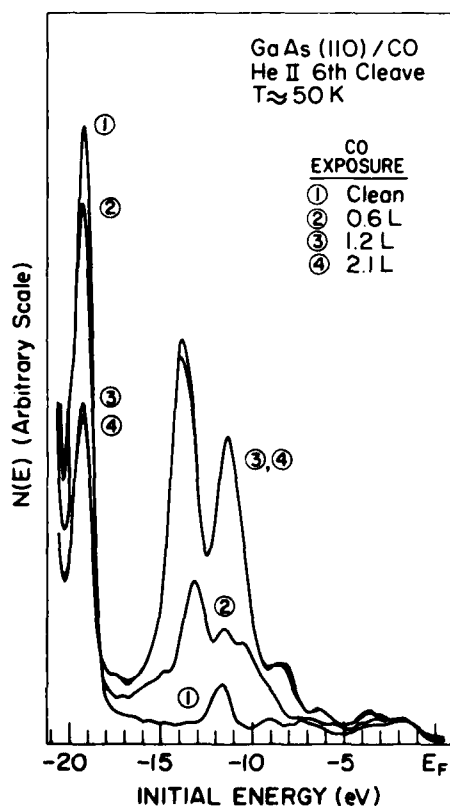


FIG. 3. He-II EDC's obtained in a sequence of CO exposures at $T = 50$ K.

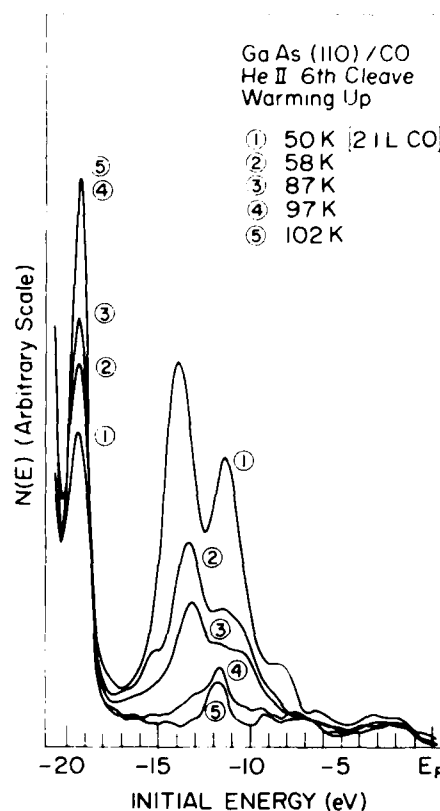


FIG. 4. Sequence of He-II EDC's obtained on warming a surface exposed to 2.1 L CO at $T = 50$ K.

Figure 5 shows the low and high coverage states in more detail. The difference curves in Fig. 5 were calculated after scaling to obtain equal count rates on the Ga 3*d* level; no shifting was required. The peaks in the high coverage state (curve 3) are tentatively assigned as indicated in the figure. The spacings between the 5*σ* and 1*π*, and the 1*π* and 4*σ* (3.15 and 2.5 eV, respectively) differ somewhat from the gas phase spacings of 2.9 and 2.8 eV.¹⁸ The 5*σ*–4*σ* spacing is essentially equal to the gas phase value. The observed spacings for the high coverage state indicate that the relaxation shift of the 1*π* level is 0.3 eV smaller than the relaxation shifts for the 4*σ* and 5*σ* levels. Only two peaks are evident in the more tightly bound low coverage state (curve 2, Fig. 5). The 2.8-eV spacing of these peaks is equal to the gas phase 1*π*–4*σ* spacing. If the two peaks are assigned to the 1*π* and 4*σ* levels then there are 1.0 and 0.8 eV increases in the relaxation shifts of the 1*π* and 4*σ* levels, respectively, as compared to the more weakly bound high coverage state. Such increases in the relaxation shift for a more tightly bound state are most likely due to increased substrate screening effects on the final state.

V. DISCUSSION

In the experiments reported here we have formed a weakly bound adlayer of molecular oxygen, yet there is no clear evidence for the formation of an appreciable amount of chemisorbed atomic oxygen until the temperature is raised and at least some oxygen desorbs. The cold-cleaved (110) surface is apparently not capable of dissociating a significant number of the weakly bound oxygen molecules. The results do

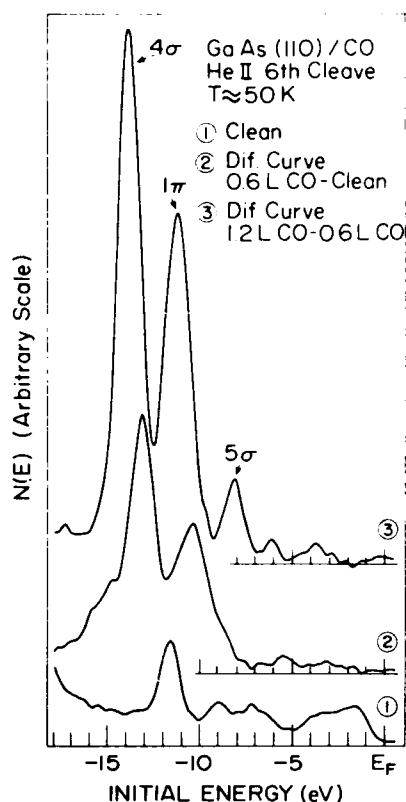


FIG. 5. He-II EDC and difference curves showing stages of CO adsorption at $T = 50$ K. Small peaks in the 3–7 eV region of curve 3 are the 4σ and 1π levels excited with 48.4 eV light.

appear to be consistent with a defect-type model for oxygen dissociation. A combination of the low temperature and the presence of the physisorbed layer of molecular oxygen may limit the mobility of the small proportion of oxygen molecules that do land on defect sites and are dissociated. As the temperature is raised and some of the oxygen is desorbed it may be possible for additional oxygen to be dissociated, move away from the defect sites, and bond to the surface. These first low temperature experiments also suggest that there may be one or more intermediate states before the formation of the chemisorbed state ordinarily generated with heavy 300 K dosing. Su *et al.*²⁰ have reported two stages in the chemisorption of oxygen on GaAs at room temperature. No connection has yet been identified between this two-state adsorption process and the intermediate states observed here during the sample warming process. Additional experiments with improved statistics and better temperature control are planned to further investigate these issues.

With regard to the question of the binding site for the chemisorbed oxygen, difference curves obtained for a surface exposed to oxygen at 50 K and then warmed to 300 K show a component of the Ga $3d$ core shifted ~ 1 eV toward greater binding energy, consistent with previous observations of asymmetric broadening of the Ga $3d$ level with heavy 300 K oxygen exposures.^{7,8} The 0.3–0.5 eV shift of the Ga $3d$ core level with respect to E_F for the 50 K O₂-exposed and

warmed case is also consistent with previous observations of shifts in E_f with heavy 300 K O₂ dosing of p -type GaAs.¹

The location of the oxygen $1\pi_c$ orbital 13.2 eV above the Ga $3d$ core level and 5.4 eV below the VBM implies a relaxation shift toward smaller binding energies of ~ 1.4 eV as compared to gas phase ionization potentials. Molecular oxygen spectra similar to those of Figs. 1 and 2 with relaxation shifts of 1.0–1.5 eV or greater have been observed in low temperature oxygen adsorption studies on other materials.^{16–18} Exposures beyond saturation (Fig. 3) cause an additional broadening of 0.2–0.3 eV.

The CO results are important both to provide a fingerprint for possible CO contamination in the oxygen experiments and as an interesting system in its own right. As noted in Sec. II, a combination of the CO background pressure and the CO associated with the O₂ dosing process may have resulted in CO exposures of up to a few tenths of a langmuir during an oxygen adsorption experiment at 50 K. However, it is difficult to observe the CO uptake in such cases due to an overlap in molecular CO and O₂ peak positions. At temperatures above 50 K, after the main molecular O₂ peaks have disappeared, we have in some cases observed shoulders near 10 and 12 eV that can be attributed to small amounts of CO in the low coverage state. Based on the RGA results and the lack of clear evidence of CO peaks in the 50 K oxygen data we estimate CO coverage to be at most 5%–10% of the O₂ coverage and hence not a major factor in the physisorption process studied here. The results also suggest that effects observed above 100 K in the oxygen experiment are not likely to be related to CO contamination. The CO–GaAs (110) system may prove to be a useful model system since it exhibits a reversible two-stage adsorption/desorption cycle. Additional techniques such as polarization-dependent angle-resolved photoemission may be able to determine symmetries and/or binding sites for the two physisorbed states.

VI. CONCLUSIONS

We have shown that O₂ and CO physisorb on cleaved GaAs (110) at 50 K. In the case of oxygen the broadened molecular O₂ peaks occur with spacings essentially equal to the gas phase values, and with a relaxation shift of ~ 1.4 eV. On warming the GaAs surface most of the oxygen desorbs by 60 K, and by 300 K the remaining oxygen is converted to the chemisorbed state. The observations indicate that the pristine (110) surface does not dissociate O₂ even with monolayer coverages of O₂ molecules on the surface.

In the case of physisorbed CO two structures are observed, a high coverage structure which desorbs by 60 K and a lower coverage structure which remains until nearly 100 K. Shifts in relative peak positions and peak heights of the two structures and the different desorption temperatures suggest two different bonding modes for the CO molecule on the (110) surface.

ACKNOWLEDGMENTS

The authors would like to acknowledge helpful discussions with J. Anderson and J. Hermanson and the technical

support of M. Jaehnig and T. Knick. Work was carried out at CRISS, an NSF Regional Instrumentation User Facility at MSU, NSF Grant No. CHE-7916134.

^aThe work was supported by AFOSR under Contract No. F49620-77-C-0125 and Grant No. 82-0267.

^bPresent Address: Jilin University, People's Republic of China.

^cPresent Address: University of Petroleum & Minerals, Dhahran, Saudi Arabia.

¹P. E. Gregory and W. E. Spicer, *Surf. Sci.* **54**, 229 (1976).

²P. Pianetta, I. Lindau, C. M. Garner, and W. E. Spicer, *Phys. Rev. Lett.* **37**, 1166 (1976).

³P. Pianetta, Ph.D. thesis, Stanford University SSRL Report 77/17.

⁴H. Luth, M. Buchel, R. Dorn, M. Liehr, and R. Matz, *Phys. Rev. B* **15**, 865 (1977).

⁵E. J. Mele and J. D. Joannopoulos, *Phys. Rev. B* **18**, 6999 (1978).

⁶J. Stohr, R. S. Bauer, J. C. McMenamin, L. I. Johansson, and S. Brennan, *J. Vac. Sci. Technol.* **16**, 1195 (1979).

⁷P. W. Chye, C. Y. Su, I. Lindau, P. Skeath, and W. E. Spicer, *J. Vac. Sci. Technol.* **16**, 1191 (1979).

⁸C. R. Brundle and D. Seybold, *J. Vac. Sci. Technol.* **16**, 1186 (1979).

⁹J. J. Barton, W. A. Goddard, and T. C. McGill, *J. Vac. Sci. Technol.* **16**, 1178 (1979).

¹⁰C. Y. Su, I. Lindau, P. W. Chye, P. R. Skeath, and W. E. Spicer, *Phys. Rev. B* **25**, 4045 (1982).

¹¹P. R. Norton, R. L. Tapping, H. P. Broida, J. W. Gadzuk, and B. J. Wacławski, *Chem. Phys. Lett.* **53**, 465 (1978).

¹²D. Schmeisser and K. Jacobi, *Chem. Phys. Lett.* **62**, 51 (1979).

¹³P. Hofmann, K. Horn, A. M. Bradshaw, and K. Jacobi, *Surf. Sci.* **82**, L610 (1979).

¹⁴R. Opila and R. Gomer, *Surf. Sci.* **105**, 41 (1981).

¹⁵D. Schmeisser and K. Jacobi, *Surf. Sci.* **108**, 421 (1981).

¹⁶G. M. Lancaster, J. A. Taylor, A. Ignatiev, J. W. Rablais, *J. Electron Spectros. Relat. Phenom.* **14**, 143 (1978).

¹⁷O. Edquist, E. Lindholm, L. E. Selin, and L. Asbrink, *Phys. Scr.* **1**, 25 (1970).

¹⁸D. W. Turner, *Molecular Photoelectron Spectroscopy* (Wiley-Interscience, New York, 1970), Chap. 3.

¹⁹R. E. Honig and H. O. Hook, *RCA Rev.*, 360 (1960).

²⁰C. Y. Su, I. Lindau, P. R. Skeath, P. W. Chye, and W. E. Spicer, *J. Vac. Sci. Technol.* **17**, 936 (1980).

UV photoemission study of low temperature oxygen adsorption on GaAs(110)^{a)}

D. J. Frankel, J. R. Anderson, and G. J. Lapeyre

Department of Physics, Montana State University, Bozeman, Montana 59717

(Received 11 April 1983; accepted 4 May 1983)

The adsorption of oxygen on the (110) cleaved surface of GaAs is studied by first physisorbing molecular O₂ on the surface at a temperature of approximately 45 K and then warming the surface to 300 K. The transformation from a state with molecular O₂ physisorbed on the surface to one with chemisorbed atomic oxygen is studied with ultraviolet photoemission spectroscopy (UPS) using a helium resonance lamp as a source. The physisorbed state shows a set of emission peaks with spacings equal to the gas phase values. The sample temperature is not cold enough to obtain multiple layers of condensed oxygen. As the temperature of the sample is then increased from $T = 45$ to 300 K, the UPS spectrum changes dramatically; by $T = 60$ K the molecular O₂ peaks have disappeared and by 170 K the spectra have taken on a form characteristic of chemisorbed atomic oxygen. Evidence is found for one or more intermediate states during the transformation of the physisorbed molecular O₂ to chemisorbed atomic oxygen.

PACS numbers: 68.45.Da, 82.65.My, 82.80.Pv

I. INTRODUCTION

The adsorption of oxygen on the GaAs(110) surface has been examined in a number of studies.¹⁻¹¹ These studies have generally been carried out at room temperature and have required rather heavy oxygen exposures because of the low sticking coefficient for oxygen on GaAs(110) at 300 K. The present interpretation of these studies is that the oxygen molecules disassociate and chemisorb atomically to the surface. In the more recent work^{10,11} evidence has been reported for the presence of more than one chemisorbed state at room temperature. However, the exact nature of the oxygen-GaAs chemisorption bond remains an open question.

In a previous paper¹² we have reported results of low temperature O₂ and CO adsorption experiments on GaAs that demonstrated that oxygen and CO physisorb to GaAs(110) at approximately 45 K with coverages of the order of a monolayer. In this article we report further data concerned with the process of converting the physisorbed molecular oxygen to chemisorbed atomic oxygen. The conversion process is investigated by first adsorbing molecular oxygen at low temperatures where the sticking coefficient is high and then studying the oxygen-GaAs system using UV photoemission as the surface is warmed to 300 K. Both oxygen-derived features in the valence band region of the photoemission spectra and the location and shape of the Ga 3*d* core are followed as a function of temperature after the initial low temperature oxygen exposures. As the sample is warmed we find that the physisorbed state evolves via an intermediate state to the state normally observed after heavy room temperature oxygen exposures. In addition we find that this intermediate state can be formed directly by exposure to oxygen at temperatures slightly above the physisorption temperature.

II. EXPERIMENTAL EQUIPMENT AND PROCEDURES

Experiments were carried out in a stainless steel ion-pumped vacuum chamber with a base pressure of

$\sim 2 \times 10^{-10}$ Torr. The chamber was fitted with a single pass cylindrical mirror analyzer (CMA) and coaxial electron gun for Auger analysis, quadrupole residual gas analyzer (RGA), UV source modeled after the design of Lancaster *et al.*,¹³ and a double pass CMA to analyze the photoemitted electrons. A special manipulator coupled to a closed cycle refrigerator allowed the sample to be moved to the various working points in the chamber while being cooled to below 50 K. Temperatures noted here were obtained from an Au-0.07% Fe vs chromel thermocouple attached to the crystal holder. Measurements with a second thermocouple attached to the crystal face with conducting epoxy indicated that, for an average length crystal, the crystal face was approximately 5 K warmer than the holder. The sample was *p*-type Zn-doped GaAs (110) from Laser Diode Laboratories with a carrier density $N \sim 3 \times 10^{18}/\text{cm}^3$.

The experiments were performed by cleaving and dosing the sample at the minimum temperature (~ 45 K) and then letting the crystal temperature rise by turning off the refrigerator. Oxygen exposures were accomplished by filling a thermocouple-gauged prechamber with a measured amount of O₂ (usually 1-10 m Torr), and injecting this dose of oxygen into the main chamber. In order to avoid the effects of excited oxygen^{2,3} the ion gauge and all other hot filaments were kept off during the actual experiments. As a result, the absolute values of the oxygen exposures are only known to within $\sim 30\%$. The rate of change of the temperature during the warmup process was such that above ~ 60 K the sample temperature increased by < 5 K during the time required to record a full energy distribution curve (EDC). Between 45 and 60 K the rate of increase of the temperature was such that it was not possible to follow the sample's behavior in detail.

In carrying out a series of experiments such as these, care must be taken to account for possible contamination with other adsorbed molecules, particularly CO. RGA measurements at 45 K show that each dose of oxygen is accompanied by a pulse of CO roughly 100 times smaller. In addition,

during the time needed to obtain several EDC's at 45 K the background pressure of CO generates an exposure of the order of a few tenths of a Langmuir. During the subsequent warming process both oxygen and CO are liberated. In control experiments with the RGA and ion gauge the analysis chamber pressure does not exceed 4×10^{-8} Torr during warming and the total exposure to desorbing CO and O_2 is less than 5 L above background. While it is difficult to completely account for the effects of CO in such an experiment, the low temperature adsorption properties of CO are known¹² and so the CO photoemission structures can, to a large extent, be separated out in the final results. Further, the total CO exposure was generally less than 10% of the total oxygen exposure.

III. OXYGEN EXPERIMENTS

Curves 1 and 2 of Fig. 1 illustrate the process of physisorbing oxygen on GaAs. Curve 1 is an angle-integrated He II EDC of low-temperature-cleaved GaAs(110). Features due to three lines of the He resonance lamp ($h\nu = 40.8, 48.4, 51.0$ eV) are evident. The peaks labeled A are due to the Ga 3d core excited with 40.8, 48.4, and 51.0 eV light. Curve 2 is obtained by subtracting the clean EDC (curve 1) from an EDC obtained after exposing the sample to 11 L O_2 at $T = 45$ K. The difference EDC exhibits a series of peaks which correspond in number and spacing to the gas phase molecular oxygen orbitals.^{14,15} The adsorption process saturates after exposures of approximately 2 L, exposures beyond saturation cause small additional increases in the oxygen peak heights coupled with a broadening of the O_2 peaks by 0.2–0.3 eV on the lower binding energy side. At 45 K the sample temperature is not cold enough to obtain multiple layers of condensed oxygen.

After preparing the saturated physisorbed state the sample temperature is allowed to increase and the conversion to the chemisorbed state is studied by following changes in valence band features and correlating them with various stages in the interaction of oxygen with the GaAs(110) surface. Curves 3–6 of Fig. 1 show the sequence of events observed when the refrigerator is turned off and the sample is allowed to slowly warm after exposures totaling 34 L O_2 at 45 K. The strong molecular oxygen peaks disappear by 60 K leaving a structure that can be identified with an intermediate state. This state, which is evident in the 60–100 K temperature range (curves 3 and 4), is characterized by two broad features centered at initial energies of 2 and 7 eV. The broad 5 eV peak characteristic of chemisorbed atomic oxygen is not evident at these temperatures.

Features at 10 and 12 eV are also observed in the 60–100 K temperature range but based on separate CO adsorption experiments¹² are attributed to a small amount of adsorbed CO. Curve 7 of Fig. 1 is a difference curve for a low coverage physisorbed CO state obtained during the separate CO experiments by exposing the sample to CO at 45 K and then warming to 77 K. The peak heights of the CO structures in curve 7 correspond to peak heights observed after exposures to CO of approximately 0.7 L at temperatures of ~ 45 K. The 10 and 12 eV peaks occurring in the oxygen experiments coincide with the CO features of curve 7, and the peaks largely disappear by about 90 K, as is the case in the CO experi-

ments. The amplitude of the peaks in curves 3 and 4 correspond to CO exposures of at most a few tenths of a Langmuir.

Beginning at a temperature of about 100 K the 2 and 7 eV peaks assigned to the intermediate state decrease in strength and the broad peak at 5 eV gradually develops. The process is largely completed by 150–170 K and results in a structure which can be identified with that observed in previous room temperature oxygen exposure studies. Auger measurements at 300 K after oxygen exposures at $T = 45$ K confirm the presence of a small amount of oxygen on the surface.

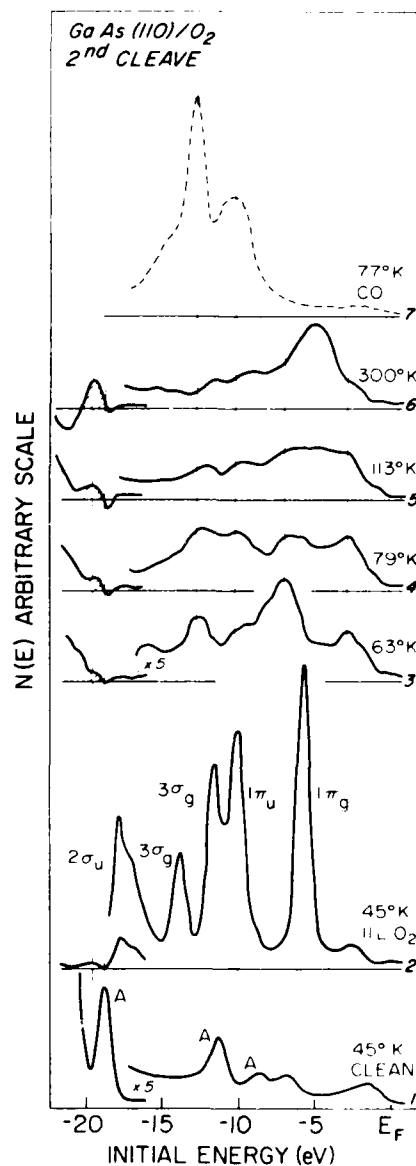


FIG. 1. Curve 1, He II EDC of clean GaAs(110); Curves 2–6, difference curves obtained by subtracting the clean EDC (curve 1) from EDC's obtained at the indicated temperatures. The EDC's have been shifted and scaled to superimpose the Ga 3d core feature prior to subtraction. Curve 7, difference curve for a low coverage CO state (see Ref. 12).

Oxygen exposure experiments have also been carried out at slightly higher temperatures (50–55 K). In these experiments the intermediate state (curve 3, Fig. 1) is formed directly and no evidence for the gas phase features (curve 2) is found. Peaks are also observed at 10 and 12 eV, but are again assigned to physisorbed CO since they also appear after holding the sample at low temperature for several hours without exposure to oxygen, and their positions and relative peak heights correspond to peaks observed in the separate CO exposure experiments. On warming samples exposed to oxygen at about 55 K behavior similar to that described above and shown in Fig. 1 is observed.

The conversion from the physisorbed to chemisorbed state may also be studied by following changes in the Ga 3d core, including shifts in its initial energy with respect to the Fermi energy and changes in its peak shape. In order to study these effects in detail all EDC's were shifted and scaled to superimpose the Ga 3d core line initial energy position and peak amplitude. The scaling was required to compensate for changes in the Ga 3d core peak height with changes in oxygen coverage, and for changes in optical alignment due to differential expansion of the manipulator on warming from 45 to 300 K. The shifting procedure allowed for an accurate (± 50 meV) measurement of shifts in the initial energy position of the main Ga 3d line with oxygen exposure and temperature as well as for an analysis of changes in peak shape.

The position of the main Ga 3d core line as a function of oxygen exposure and temperature is shown in Fig. 2. A shift in the core of ~ 0.1 eV towards E_F is observed after the initial oxygen exposure. The shift is observed after exposures as low as 0.5 L and its size is independent of the magnitude of the exposure. The position of the Ga 3d core level and the VBM with respect to E_F remain essentially unchanged as the sample is then allowed to warm to 60 K. In the 60–100 K temperature range, where the intermediate state is observed in the valence band data, the Ga 3d core shifts slightly (0.05–

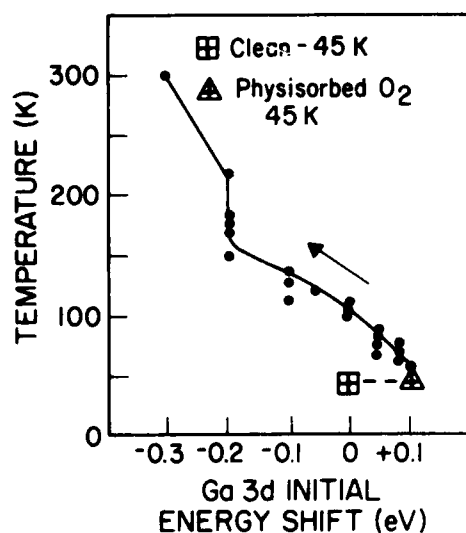


FIG. 2. Initial energy value of Ga 3d photoemission level as a function of temperature following exposure to oxygen at $T = 45$ K. The square denotes the position of the Ga 3d for clean GaAs(110), the triangle the value immediately after exposure to oxygen, and the dots the values as the crystal's temperature increases to 300 K.

0.1 eV) away from E_F . As the temperature is then increased from 100 to 300 K the Ga 3d core broadens and continues to shift further away from the Fermi energy. At 300 K the Ga 3d initial energy position shows a net shift of ~ 0.3 eV towards greater binding energy as compared to the cold-cleaved and still undosed case. A similar shift is seen in the VBM. The origin of the initial 0.1 eV shift towards E_F on oxygen adsorption remains uncertain as the position of the VBM cannot be measured with as high an accuracy as that of the Ga 3d core, and it is thus not possible to differentiate between a chemical shift and band bending effects. The subsequent larger 0.3 eV shift of the Ga core away from E_F is most likely due to band bending effects as the shift is roughly paralleled by changes in the VBM position. A similar shift in the location of E_F for *p*-type GaAs(110) has previously been reported following heavy 300 K oxygen exposures.

In addition to the shifts in location of the main Ga 3d line (Fig. 2) which are most likely due to band bending effects, we have also observed changes in the shape of the Ga 3d core. These changes in shape can be attributed to the growth of a small chemically shifted component of the core line. The difference curves 2–6 of Fig. 1 which are obtained from the shifted and scaled EDC's are useful in examining these changes in the shape of the Ga 3d core with increasing temperature. The curves show the growth of a component of the core shifted by approximately 1 eV toward deeper binding energy. In Fig. 1, the two vertical lines note the positions of the main core line (zero amplitude in difference curve), and of the shifted line which is shown shaded.

The concentration of oxygen on the crystal surface is an important question. The saturation behavior observed at 45 K is strong evidence for an oxygen coverage of about a monolayer in the initial physisorbed state. Unfortunately, it is difficult to monitor the amount of oxygen present on the surface as the sample warms from 45 to 300 K. The relative peak areas of the valence oxygen features can give some indication. As shown in Fig. 1, the peak areas of the oxygen features of the intermediate state and the 300 K chemisorbed state are considerably smaller than for the saturated physisorbed state. A similar indication is provided by the area under the shifted portion of the Ga 3d core, which is at most 10%–20% of the area under the main peak. Finally, Auger measurements can provide some information but must be used with caution because of possible interactions of the electron beam with the sample, including electron-induced desorption and surface damage. Presently, the 300 K Auger measurements suggest somewhat lower oxygen coverages than is implied by the UPS peak area considerations.

IV. DISCUSSION

The experiments show that there is an intermediate state present prior to the formation of the chemisorbed state ordinarily generated with heavy 300 K oxygen exposures. The 300 K state has been assigned to chemisorbed atomic oxygen and is characterized by a broad peak at 5 eV, several weaker features in the 8–12 eV range, the presence of a shifted component in the Ga 3d, and a shift in the location of the main Ga 3d peak of ~ 0.3 eV away from the Fermi energy as compared to clean GaAs. In contrast at temperatures of 60–100

K we observe a state characterized by broad features centered at ~ 2 and 7 eV, a smaller shifted component of the Ga $3d$, a small (< 0.1 eV) shift in the location of the main Ga $3d$ peak, and the absence of a strong feature of 5 eV. This intermediate state is produced either by first physisorbing molecular O_2 at 45 – 50 K and then warming to 60 – 100 K or by direct oxygen exposure at temperatures just above the physisorption temperature. The reduced magnitude of the shifted Ga $3d$ and the absence of a strong 5 eV peak, together with the assignment of the 300 K state to chemisorbed atomic oxygen suggest that the intermediate state may be due to chemisorbed molecular oxygen.

There remains some question as to whether this intermediate state characterized by the pair of peaks is one simple state since the temperature evolution of the 2 and the 7 eV peaks do not exactly coincide. Figures 1 and 2 show that the conversion from the intermediate state to the 300 K state occurs gradually. It is therefore possible that there is a small admixture of the 300 K state in the 60 – 100 K temperature range. A second interpretation is that there is more than one intermediate state. The existence of several intermediate states cannot be ruled out since the strong molecular O_2 peaks present at temperatures of 45 – 55 K could mask features due to a small amount of such a state. Further, the rapid temperature rise from 45 to 60 K complicates analysis of the data during the initial stages of the warming when such a state might be observed.

A two-stage adsorption process for oxygen at room temperature has been reported^{10,11} and also has been observed by our group in synchrotron radiation studies of 300 K oxygen adsorption. The two states are differentiated by the presence or absence of a peak near 10 eV together with weaker features in the 6 – 8 eV region. Both states exhibit a strong peak near 5 eV. Unfortunately, the presence of the CO-derived peaks in the 8 – 12 eV range of our spectra together with features (peaks A in Fig. 1) arising from excitation of the Ga $3d$ core level by light of energy $h\nu = 48.4, 51.0$ eV makes it difficult to look for or follow weak oxygen-derived features in this energy range. The absence of a strong peak at 5 eV in the 60 – 100 K temperature range does, however, suggest that the intermediate state is a different state than that observed at 300 K. Direct comparisons with the theoretical work of Mele and Joannopoulos⁵ are also complicated by the CO and Ga structures in the 8 – 12 eV range of our spectra since the peaks described by Mele and Joannopoulos as differentiating between chemisorbed O_2 and O are unfortunately also found in this energy range.

In low temperature oxygen exposure experiments on gallium surfaces, Schmeisser and Jacobi¹⁶ have identified an intermediate state present at ~ 70 K which is characterized by a strong peak at 5 eV, a doublet at 9 and 10.3 eV and a shifted component of the Ga $3d$ core. They assign this structure to O_2 chemisorbed on the gallium. There is a superficial similarity between this state and the two-peaked structure

with peaks separated by ~ 5 eV observed for the intermediate state of oxygen on GaAs. However, it is not yet possible to draw any firm conclusions on the relation of these two states.

VI. CONCLUSIONS

We have used UPS to observe molecular oxygen physisorbed to GaAs(110) at low temperatures and followed its transformation to chemisorbed atomic oxygen at room temperature. At temperatures below 50 K we observe broadened molecular O_2 peaks with spacings essentially equal to gas phase values after exposures of less than a Langmuir of oxygen. Between 50 and 100 K we observe at least one distinct intermediate state of oxygen on GaAs and above 100 K observe the gradual formation of chemisorbed atomic oxygen. The intermediate state has also been observed after oxygen exposures at temperatures just above the physisorption temperature.

The observations indicate that chemisorbed atomic oxygen is not formed directly with oxygen exposures at low temperature and that there is at least one intermediate form of oxygen on GaAs, possibly chemisorbed molecular oxygen.

ACKNOWLEDGMENTS

The authors would like to acknowledge helpful discussions with J. Hermanson and the technical support of M. Jaehrig and T. Knick. Work was carried out at CRISS, an NSF Regional Instrumentation User Facility at MSU, NSF Grant No. CHE-7916134.

⁴The work was supported by AFOSR under Grant No. 82-0267 and by NSF Grant No. DMR-8205581.

¹P. E. Gregory and W. E. Spicer, *Surf. Sci.* **54**, 229 (1976).

²P. Pianetta, I. Lindau, C. M. Garner, and W. E. Spicer, *Phys. Rev. Lett.* **37**, 1166 (1976).

³P. Pianetta, Ph.D. thesis, Stanford University (1976) SSRL Report 77/17.

⁴H. Luth, M. Buchel, R. Dorn, M. Liehr, and R. Matz, *Phys. Rev. B* **15**, 865 (1977).

⁵E. J. Mele and J. D. Joannopoulos, *Phys. Rev. B* **18**, 6999 (1978).

⁶J. Stohr, R. S. Bauer, J. C. McMenamin, L. I. Johansson, and S. Brennan, *J. Vac. Sci. Technol.* **16**, 1195 (1979).

⁷P. W. Chye, C. Y. Su, I. Lindau, P. Skeath, and W. E. Spicer, *J. Vac. Sci. Technol.* **16**, 1191 (1979).

⁸C. R. Brundle and D. Seybold, *J. Vac. Sci. Technol.* **16**, 1186 (1979).

⁹J. J. Barton, W. A. Goddard, and T. C. McGill, *J. Vac. Sci. Technol.* **16**, 1178 (1979).

¹⁰C. Y. Su, I. Lindau, P. R. Skeath, P. W. Chye, and W. E. Spicer, *J. Vac. Sci. Technol.* **17**, 936 (1980).

¹¹C. Y. Su, I. Lindau, P. W. Chye, P. R. Skeath, and W. E. Spicer, *Phys. Rev. B* **25**, 4045 (1982).

¹²D. J. Frankel, Y. Yu-ken, R. Avci, and G. J. Lapeyre, *J. Vac. Sci. Technol.* **A 1**, 679 (1983).

¹³G. M. Lancaster, J. A. Taylor, A. Ignatiev, and J. W. Rablais, *J. Electron Spectrosc. Relat. Phenom.* **14**, 143 (1978).

¹⁴O. Edquist, E. Lindholm, L. E. Selin, and I. Asbrink, *Phys. Scr.* **1**, 25 (1970).

¹⁵D. W. Turner, *Molecular Photoelectron Spectroscopy*, (Wiley Interscience, New York, 1970), Chap. 3.

¹⁶D. Schmeisser and K. Jacobi, *Surf. Sci.* **108**, 421 (1981).

Photoemission study of GeAs($\bar{2}01$): A model for the As-stabilized Ge surface on GaAs/Ge heterojunctions^{a)}

F. Stucki and G. J. Lapeyre

Department of Physics,^{b)} Montana State University, Bozeman, Montana 59717

Robert S. Bauer, P. Zurcher, and J. C. Mikkelsen, Jr.

Xerox Palo Alto Research Center,^{c)} Palo Alto, California 94304

(Received 26 January 1983; accepted 12 May 1983)

We present a study of the electronic states of GeAs as a model for the ordered, anion-stabilized surface phases which form on Ge when it is grown epitaxially on GaAs substrates using MBE. Angle-resolved, normal emission photoelectron energy distribution curves for four different azimuthal orientations of the GeAs($\bar{2}01$) face (i.e., four different polarizations) have been measured using photon energies from $h\nu = 10$ to 28 eV. The valence band structure plots (binding energy versus photon energy) show behavior typical of a layered compound. A large number of valence band states (about 12) are observed, and they show essentially no $h\nu$ dispersion in normal emission and very little dispersion with polar angle. The electronic states are therefore localized both within and normal to the layer. The excitation of the Ge $3d$ and the As $3d$ core levels into conduction band states observed by measuring the core hole decay emission does not show any enhancement peaks as usually observed if empty surface states exist in the conduction band. This suggests that the GeAs($\bar{2}01$) surface may not have any surface states. Chemical bonding information was obtained by measuring the Ge $3d$ core level binding energy. The Ge is more tightly bound compared to the bulk Ge as indicated by a $3d$ core level chemical shift of 0.45 ± 0.1 eV toward higher binding energy. $3d$ core threshold emission for both the Ge and the As is used together with the line shape of the valence band edge emission to determine a forbidden band gap is 0.4 ± 0.3 eV. These results support the Bauer/Mikkelsen hypothesis that the Ge:As surface phase that floats on top of the MBE GaAs/Ge heterojunction is energetically more favorable than the corresponding clean Ge surface having unsatisfied dangling bonds. The data on GeAs($\bar{2}01$) leads to a picture of an As-terminated surface having highly directional orbitals and very low reactivity.

PACS numbers: 73.20. - r, 73.40.Lq, 68.55. + b, 68.60. + q

I. INTRODUCTION

During the MBE growth of epitaxial, lattice-matched Ge on GaAs, stability of the interface chemical nanostructure is achieved only after As diffuses to the free Ge surface.¹ Monch and Gant² first reported the presence of an ordered layer of As on the surface of Ge that is thermally evaporated onto a cleaved GaAs(110) substrate at epitaxial temperatures.³ Upon further studies using MBE, we have reported this occurring on all the low index faces of GaAs; it is a general phenomena occurring for $325^\circ \pm 25^\circ\text{C}$ growth on starting substrates ranging from stoichiometric GaAs(110)(1×1), to the As-rich GaAs(100) $c(4 \times 4)$, $c(2 \times 8)$ and GaAs(111)(2×2) surfaces, and the Ga-rich GaAs(100) 4×6 surface.⁴ Detailed LEED studies of the (100) grown faces have confirmed the presence of these ordered As surface layers.⁵ This anion outdiffusion does not occur during the initial chemisorption of Ge; rather, using soft x-ray photoelectron spectroscopy, we measure a rearrangement of Ge for As during the intermediate stages of heterojunction formation.¹ GeAs_x forms ordered 3×1 , two domain (1×2) , and (1×1) phases at the free surface of Ge(110), Ge(100), and Ge(111) on the respective GaAs orientations. The GeAs_x - $(1 \times 2) + (2 \times 1)$ ordered Ge(100):As surface phase

is compositionally and structurally independent of the initial GaAs(100) surface As concentration.¹ Furthermore, the final Ge:As surface concentration is the same as for MBE GeAs_x layers grown on the same crystallographic face under the same conditions.⁴

It is believed that a detailed understanding of the structural and electronic properties of these Ge:As surface phases will provide important understanding of the energetics and kinetic driving forces which control the MBE process and possibly the resulting interface electronic properties. Therefore, we have investigated the *in situ* cleaved GeAs($\bar{2}01$) surface by means of angle-resolved synchrotron photoemission spectroscopy. This bulk crystal provides a model system for the local bonding and properties of the As-stabilized Ge structures.

II. EXPERIMENTAL

The experiments were performed at the Synchrotron Radiation Center at the University of Wisconsin using the 240 MeV Tantalus II storage ring and a stainless steel Seya monochromator. To analyze the photoemitted electrons, we used an adjustable 6 in. double pass cylindrical mirror analyzer (CMA), which is modified to permit the angle-resolving ca-

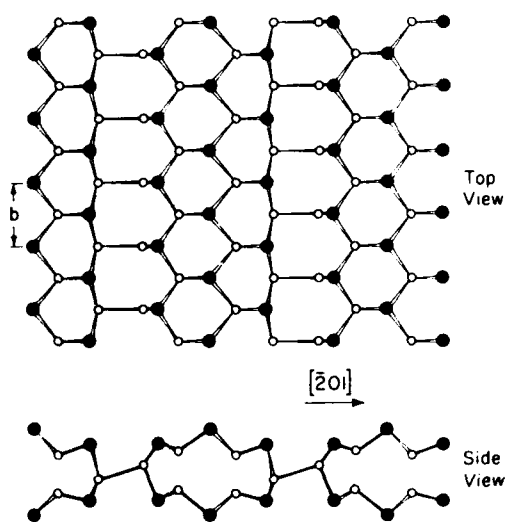
pability. By means of a rotary/linear feedthrough, we have the possibility to bring a drum with two small holes ($\pm 2^\circ$, $\pm 6^\circ$, respectively) in its side into the detected electron beam. The drum blocks all of the electron flux except that passed by the selected aperture in the cylindrical surface of the drum. By rotating the drum, any segment of the electron cone can be selected, i.e., we are able to measure at different polar and azimuthal angles.⁶

The resolution for the pass energy we used for these measurements ($E_p = 15$ eV) is 0.3 eV. We normalized the counting rate for a constant beam current measured from a W mesh through which the photon beam always passes. The energy of the photoelectrons is measured with respect to the vacuum level. The measurements were made at room temperature, and the base pressure of the system was smaller than 1.5×10^{-10} Torr. Auger spectra were obtained and no impurity elements were found.

GeAs is a layered compound and crystallizes in the monoclinic GaTe structure.⁷ A model picture (not in scale) of the ($\bar{2}01$) surface is given in Fig. 1. The surface unit cell contains 14 atoms. The GeAs single crystal was *in situ* cleaved, and the azimuthal position of the sample was determined by LEED. The LEED pattern of the clean GeAs($\bar{2}01$) surface is a $c(6 \times 2)$ as shown in Fig. 2 for 100 eV primary energy.

The azimuthal zero or 180° ($\beta = 0^\circ$, 180° , respectively) is defined by the LEED rows (i.e., the sample direction in which the spots are closely spaced in Fig. 2) being perpendicular to the light A vector. Using the two rotations of the sample manipulator, we have the possibility to rotate the sample around the sample surface normal as well as to change the polar angle of the incident light.

We measured the angle-resolved energy distribution curves (AREDC) for electrons emitted normal to the surface for four different polarizations ($\beta = 0^\circ, 90^\circ, 180^\circ, 270^\circ$) of the GeAs($\bar{2}01$) surface using 18 values of photon energy from $h\nu = 10$ to 28 eV. A combined azimuthal polar angle depen-



GeAs: ($\bar{2}01$) layer structure

FIG. 1. Model representation (not to scale) of the side and top views of the GeAs layered structure. The full circles represent threefold coordinated As and the open circles represent fourfold coordinated Ge atoms.



FIG. 2. LEED photograph of the $c(6 \times 2)$ structure of the ($\bar{2}01$) layered face of the GeAs crystal used in this study for 100 eV primary electrons.

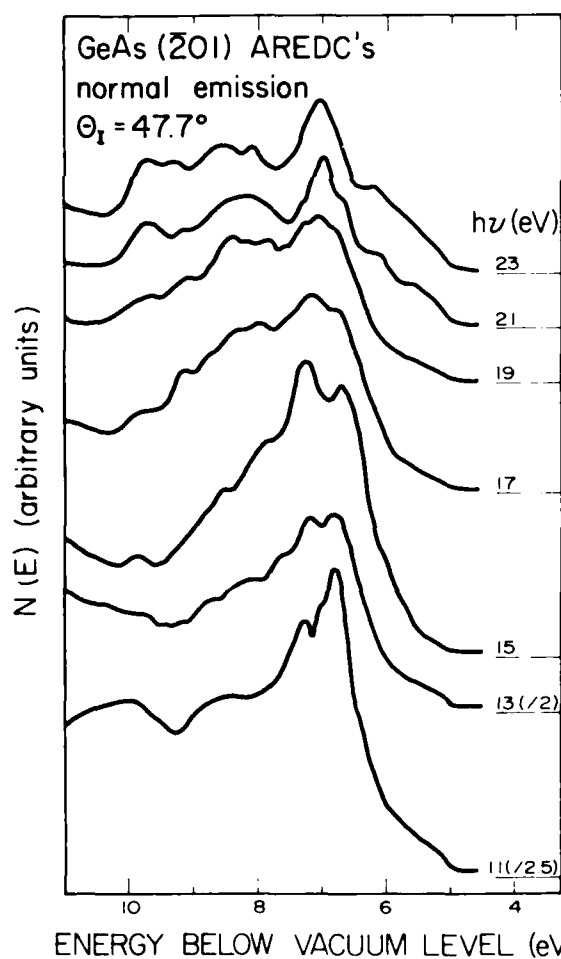


FIG. 3. Photon energy dependence of the angle-resolved electron distribution curves (AREDCs) for GeAs($\bar{2}01$). This data was taken for the light vector perpendicular to the LEED rows (i.e., $\beta = 0^\circ$) which places A parallel to "b" dimension in Fig. 1). The amplitude of the $h\nu = 13$ and 11 eV AREDC's are reduced by 0.5 and 0.4, respectively.

dependency of AREDC's at a photon energy of 16 eV was measured for $\beta = 0$ by rotating the CMA angle-resolving drum. Note that the CMA symmetry axis makes an angle of 45° with respect to the crystal normal. The $3d$ core threshold emission for both the Ge and the As core as well as the binding energy of the Ge core were also measured.

III. RESULTS

The results of the sets of normal emission AREDC's for the four polarizations are summarized by a set of selected AREDC's in Fig. 3 and the structure plot of Fig. 4. The AREDC's in Fig. 3 illustrate nicely the complexity encountered in analyzing the data. The three peaks at 6.8, 7.0, and 7.3 eV below the vacuum level, for example, change their relative intensities rather dramatically with $h\nu$. For $h\nu = 11$ eV, the peak at 6.8 eV is strong. The middle peak makes only a shoulder, and the peak at 7.2 eV is weak. For $h\nu = 15$ eV, the peak at 7.3 eV is strong, the middle peak is not resolved, and the peak at 6.8 eV is weak. At higher photon energies the middle peak is stronger. For example, for $h\nu = 19$ eV, the peaks at 6.8 and 7.3 eV are only weak, and for $h\nu = 23$ eV,

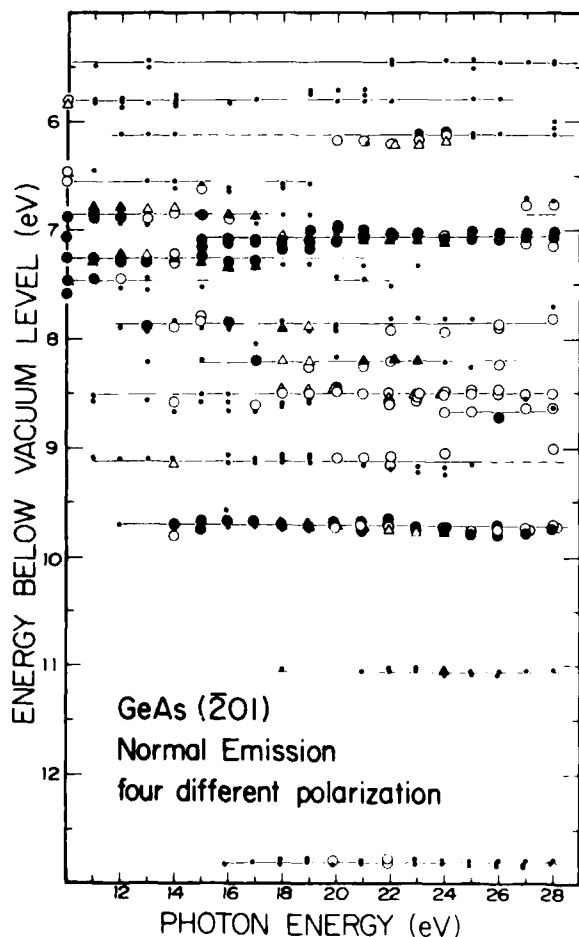


FIG. 4. Composite plot of the positions of structures observed in normal emission AREDCs. The intensity is represented schematically by the use of full circles and triangles correspond to strong structures, open circles to weak peaks, and dots to shoulders. The triangles which correspond to the data in Fig. 3 (i.e., $\beta = 0^\circ$) while the circles show positions at the other polarizations used in these studies (i.e., $\beta = 90^\circ, 180^\circ, 270^\circ$).

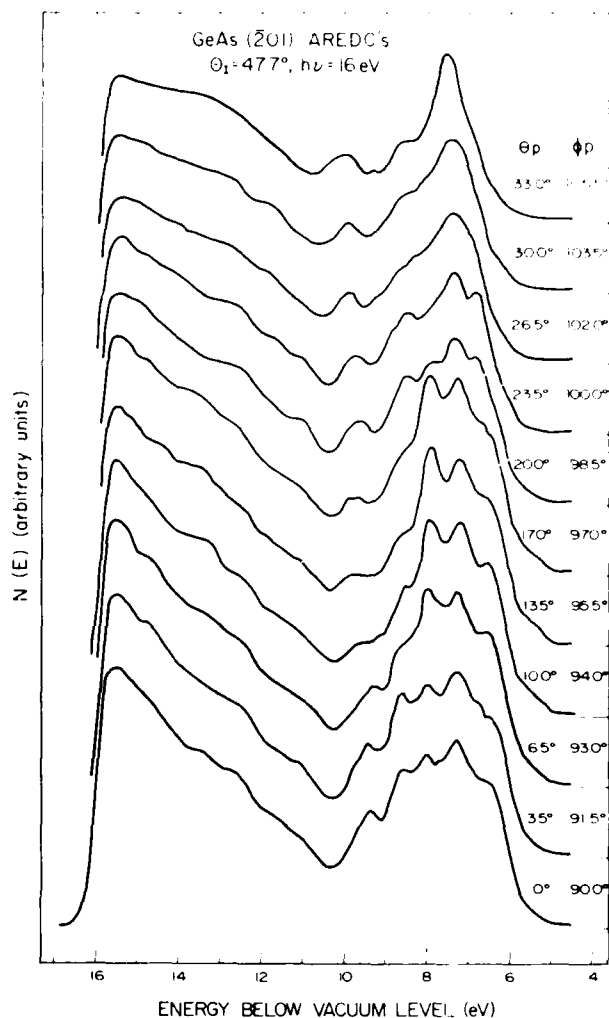


FIG. 5. Electron emission angle dependence of the AREDCs for GeAs(201). This data was taken for the detector polar (Θ_p) and azimuthal (Φ_p) angles shown with the light kept at a constant photon energy (16 eV) and orientation relative to the sample ($\beta = 0^\circ$).

we are not able to resolve the two outer peaks. In such analysis it is often difficult to make the decision by looking at only one set of data if we have different peaks or one single peak which undergoes a shift in energy position.

Perhaps the best way to display the results is to show a structure plot constructed from all the AREDC's. The result of doing this is shown in Fig. 4. The triangles represent the peaks of the AREDC's shown in Fig. 3. The circles represent the three other polarizations. The full circles and triangles belong to strong peaks, the open circles or triangles to weak peaks, and the dots to shoulders in the AREDC's. By over-viewing the data in this way, one sees a consistency in that the AREDC peaks show a large number of flat bands.

We can also study the k -parallel dependence by rotation of the drum aperture positions. Figure 5 shows AREDC's at a photon energy of 16 eV. The polar angle varies from 0° to 33.0° and the azimuthal angle from 90° to 105.5° . The corresponding structure plot is shown in Fig. 6 (full circles: strong peaks, open circles: weak peaks, dots: shoulders).

The normal emission structure plots show no k -perpendicular dependence, a behavior typical of a layer compound.

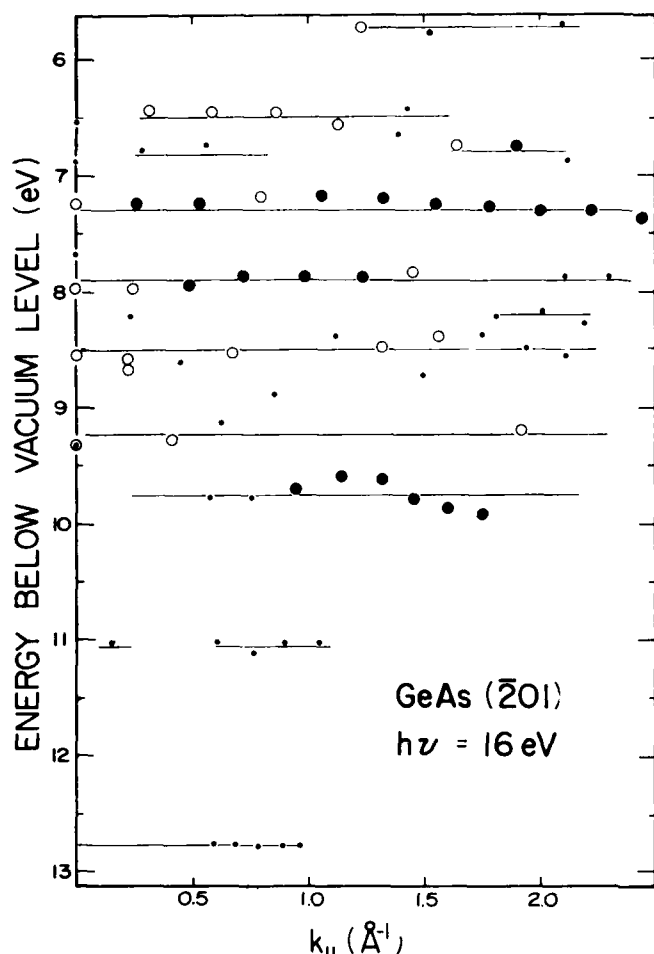


FIG. 6. Composite plot of the positions of structures observed in the electron emission-angle dependent AREDCs of Fig. 5. The intensity is represented schematically as described in Fig. 4. The structures can be related to the parallel component of the electron momentum (which is conserved during the escape into vacuum) by using the photon energy and the emission angle.

We observed a large number of valence band states (about 12), and they show very little dispersion with the polar angle, i.e., no k -parallel dependence per Fig. 6. This indicates highly localized states with nearly one "band" per atom in the large unit cell.

Around 5.5 eV below the vacuum level, we found a foot in the spectrum (e.g., Fig. 5, $\theta_p = 10.0^\circ$). There is some question as to whether that foot is an intrinsic valence band structure originating from GeAs or if it is associated with impurities or defects. At present we choose the onset of this foot as the limit for the position of the valence band maximum.

Zurcher/Bauer⁸ found a very similar valence band maximum (VBM) onset for an As-saturated Ge(110) surface. They correlated this structure with the presence of a GeAs₂ surface/interface compound. This similarity supports our assumption that the VBM in GeAs($\bar{2}01$) is at the onset of this foot.

The excitation of the Ge 3*d* and the As 3*d* core levels into conduction band states, observed by measuring the core hole decay emission, does not show any enhanced peaks as usually observed in the presence of empty surface states (see Fig. 7). This suggests that the GeAs($\bar{2}01$) surface does not have any empty surface states. Figure 7 shows a constant final

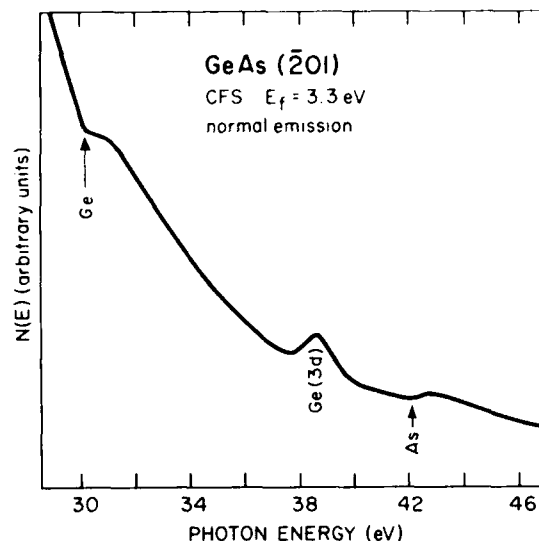


FIG. 7. The photon energy dependence of the electron emission normal to the GeAs($\bar{2}01$) surface with the final state energy of the electrons held constant at 3.3 eV kinetic energy (i.e., in the secondary electron tail of the energy distribution).

state energy spectra (CFS) for a final state energy of 3.3 eV. The Ge threshold is at 30.4 ± 0.2 eV and the As threshold at 42.4 ± 0.2 eV. The difference between the Ge- and the As-threshold energy is 12.0 ± 0.3 eV. We found the Ge 3*d* core level 35.3 ± 0.1 eV below the vacuum level by measuring EDC's as well as CFS's. The bottom of the conduction band lies 4.9 ± 0.2 eV below the vacuum level as calculated from the difference between the Ge 3*d* core level energy and the Ge threshold energy. This quantitative result assumes that electronic initial and final state relaxation effects associated with the different excitation processes for AREDC's versus CFS's are not significantly different for these two cases.

IV. DISCUSSION

The distinguishing feature of the As-terminated Ge layer seen in Fig. 1 is the presence of As lone-pair orbitals at the surface. These terminating surface bonds should be compared to the situation on the clean Ge surface. The (110), (100), and (111)Ge surfaces can be expected from theory to have large surface reconstructions to reduce the large surface energy associated with dangling bonds. Still the reconstructed surfaces are characterized by unsaturated dangling bonds. These provide sites for a reactivity to foreign atoms, a large surface strain,⁹ and the electronic states would contain evidence for surface state features.

For GeAs($\bar{2}01$) on the other hand, the surface is characterized by lone pairs which are rather inert. These are the results of slight rearrangement in the bonds which produce a large unit cell. Therefore, in our angle-resolved photoemission study we observed a large number of valence band states. There is rich change in the spectra as the photon energy and polarizations are varied. However, as summarized in the structure plots, the spectral features show essentially no $h\nu$ dispersion in normal emission and very little dispersion with polar angle. The electronic states are therefore localized within each layer.

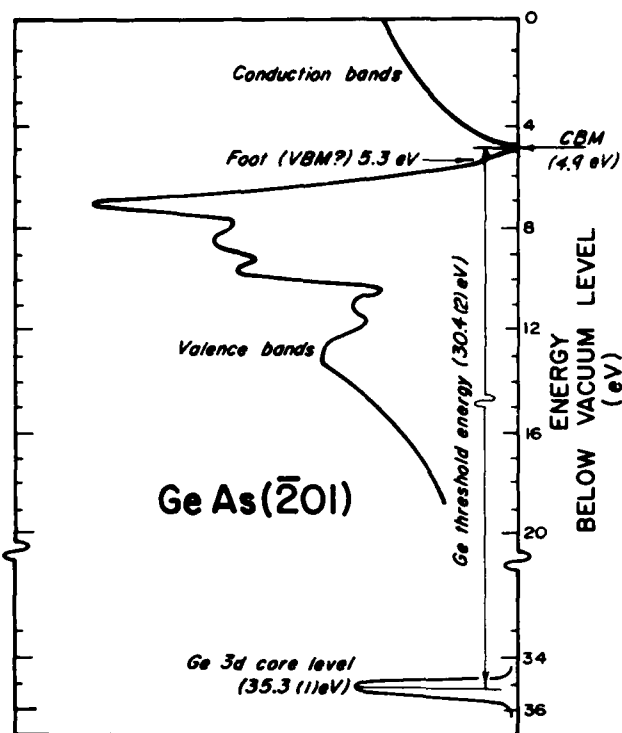


FIG. 8. Composite overview of the positions of the Ge(3d) core level, valence band density of states, valence band maximum (VBM), and conduction band minimum (CBM) obtained from the energy distribution curves (Figs. 3 and 5) and constant final state data (Fig. 7).

The absence of any strong peaks in the CFS spectrum (sometimes called partial yield) due to 3d core-to-conduction band excitations suggests that the GeAs(201) surface may not have any empty surface states. The spectra are also very insensitive to contamination, supporting a picture having at best only weak empty surface states. One of the main interests in comparing the GeAs surface to the As-stabilized Ge surface is to determine the electronic energy and role of the As lone pairs. Because we observe no states in the band gap, we speculate that the As lone pair states must represent one of the three prominent structures seen in the AREDCs. The terminating As orbitals would then be very tightly bound.

We can combine the general density of states features seen in the AREDCs with the constant final state spectra to obtain an overview of the electronic states of GeAs. By plotting these results together in Fig. 8, we obtain a measure of the energy gap of GeAs. The maximum energy of the foot in the AREDCs is 5.3 ± 0.1 eV. If the foot is an intrinsic valence band structure, then it defines the VBM. This then provides an estimate for the band gap when combined with the CFS threshold. Based on such analysis, the value for the forbidden band gap of GeAs(201) is 0.4 ± 0.3 eV. Recall that this ignores possible final state relaxation effects in the photoemission which could change this gap value. Our result is in reasonable agreement with the indirect band gap of 0.65 eV found by optical studies.¹⁰

Chemical bonding information was obtained by measuring the Ge 3d core level binding energy. The Ge is more tightly bound compared to the clean Ge as indicated by a 3d core level chemical shift of 0.45 ± 0.1 eV toward higher

binding energy [$E_B^{Ge}(Ge\ 3d) = 29.55$ eV,⁴ $E_B^{GeAs}(Ge\ 3d) = 30.0 \pm 0.1$ eV].

V. SUMMARY

When Ge heterojunctions are grown on GaAs by MBE under epitaxial growth conditions, the surface of the Ge exhibits an ordered surface phase which is stabilized by a monolayer or more of As.⁴ This GeAs_x layer has a constant composition *x* for all the principle crystallographic directions and a superstructure relative to the bulk geometric structure [e.g., a (1 × 2) relation to the growing, epitaxial Ge film for all GaAs(100) starting stoichiometries]. The As diffusion from the interface region, while lowering the free energy of the growing Ge surface layers, concurrently changes the band gap offset.¹² For example, the GaAs/Ge(100) hole barrier increases by nearly 0.5 eV when As abruptly leaves the interface and diffuses through the Ge thin film, causing the ordered surface. Therefore, we have studied the inert, layered (201) surface of GeAs as a model for the GeAs_x layer whose formation correlates with the ultimate GaAs/Ge band gap discontinuity.¹

The electronic states of the model GeAs surface are localized within the layered structure. It is characterized by highly directional orbitals and no observable surface states. Contamination tests of the spectra show no changes. This is consistent with the lack of discernable surface states and the unreactivity of the surface.

These results are consistent with the energetic arguments previously made by Bauer and Mikkelsen¹ for the formation of GaAs/Ge heterojunctions. In particular, the "floating" GeAs_x layer enhances the stability of the growing heterojunction compared to clean Ge surfaces. Furthermore, this As capping layer provides a less reactive top surface during the MBE growth than the pure Ge would.

It is clear from our work that such model compound studies can be very important to understanding growth of interfaces and the interrelationship of the electronic and geometric structure of surfaces. What is now needed are theoretical calculations which would allow more detailed analysis of the electronic properties reported here and future LEED studies¹³ of the GeAs(201) c(6 × 2) phase to establish the geometric structure of the surface As termination. Such simple values as the relative electronic energy of the surface As lone pair states and their symmetry would be most valuable. A calculation for the origin of the band gap difference for GeAs compared to Ge would be very valuable for interpreting possible Fermi level pinning at the free surface of growing GaAs/Ge heterojunctions. In general, one hopes that theoretical work will address the central issues of surface versus interface energies that occur due to relaxation, strain, defects, local electrostatic imbalances, etc.

ACKNOWLEDGMENTS

We gratefully acknowledge the technical support of the staff of the Synchrotron Radiation Center at the University of Wisconsin in Madison and F. Hulliger for providing crystallographic information on GeAs.

^aThis paper was presented at the 10th Annual Conference on the Physics and Chemistry of Semiconductor Interfaces.

^bPart of this work was performed at Synchrotron Radiation Center of the Physical Sciences Laboratory of the University of Wisconsin, which is supported by NSF Grant No. DMR-7415089. The Montana work was sponsored by the Air Force Office of Scientific Research under Contract No. F49620-77-0125; Grant No. 820267 and under NSF Grant DMR 820558.

^cThe Xerox work is partially funded by the ONR (L. R. Cooper), contract N00014-81-C-0696.

¹R. S. Bauer and J. C. Mikkelsen, Jr., *J. Vac. Sci. Technol.* **21**, 491 (1982).

²W. Monch and H. Gant, *J. Vac. Sci. Technol.* **17**, 1094 (1980).

³R. S. Bauer and J. C. McMenamin, *J. Vac. Sci. Technol.* **15**, 1444 (1978).

⁴R. S. Bauer, *J. Vac. Sci. Technol. B* **1**, 314 (1983).

⁵B. J. Mrstik, *Surf. Sci.* **124**, 253 (1983).

⁶J. A. Knapp, G. J. Lapeyre, N. V. Smith, and M. M. Traum, *Rev. Sci. Instrum.* **53**, 781 (1982).

⁷F. Hulliger, *Structural Chemistry of Layer-Type Phases* (D. Reidel, Dordrecht-Holland, 1976); W. B. Pearson, *Handbook of Lattice Spacings and Structure of Metal and Alloys* (Pergamon, New York, 1967), Vol. 2.

⁸P. Zureher and R. S. Bauer, *J. Vac. Sci. Technol. A* **1**, 695 (1983).

⁹R. S. Bauer, *Thin Solid Films* **89**, 419 (1982).

¹⁰J. W. Rau and C. R. Kannewurf, *Phys. Rev.* **B3**, 2581 (1971).

¹¹E. A. Kraut, R. W. Grant, J. R. Waldrop, and S. P. Kowalczyk, *Phys. Rev. Lett.* **44**, 1620 (1980).

¹²R. S. Bauer and H. W. Sang, Jr., *Surf. Sci.* (in press).

¹³A. Kahn, J. Carelli, and R. S. Bauer (to be published).